JAERI 1042

Stability Analysis of Control System for British Type Power Reactors

1963年2月

日本原子力研究所

Japan Atomic Energy Research Institute

621. 039. 516. 2

Stability Analysis of Control System for British Type Power Reactors

Abstract

Since the British type power reactor is unstable due to the positive temperature coefficient of reactivity, special considerations are required in the design of the control system for this type of power reactors. Stability analyses of the system are made assuming five different types of control:

a) continuous control
b) continuous control with saturation
c) discontinuous control
d) continuous control with tachometer feedback
e) continuous control with rod position feedback

The generalized Nyquist's stability criterion and Kochenburger's describing function method are applied and the conclusions obtained are:

(1) The continuous system is unstable, when the controller gain is either too high or too low.

(2) The saturation in the control rod speed does not affect the system response significantly.

(3) When the discontinuous control is adopted, the system either diverges or undergoes sustained oscillations, corresponding to the stable limit cycles.

(4) Introduction of tachometer feedback little affects the system stability.

(5) System responses are improved by application of rod position feedback.

Analog computer studies are also included in order to ascertain the results obtained by the analytical method.

September, 1962

N. SUDA, J. MIIDA

英国型動力炉
温度制御系の安定性解析

要　　旨

英国型動力炉は正の温度係数のために不安定になるので，この型の原子炉の制御系の設計には特別の考慮が必要となる．ここでは次の5通りの制御方式を想定して，制御系の安定性の解析をおこなった．

a) 連続制御
b) 飽和特性を含む連続制御
c) 不連続制御
d) 速度フィードバックを含む連続制御
e) 位置フィードバックを含む連続制御

一般化した Nyquist の安定判別法および Kochenburger の記述関数法を応用して解析した．得られた結論は，

(1) 連続制御系はゲインが高すぎても，また低すぎても不安定になる．
(2) 制御棒速度の飽和特性は系の応答にそれほど大きい影響をおよぼさない．
(3) 不連続制御方式では系は発散するか，または安定なリミットサイクルに相当する持続振動をする．
(4) 速度フィードバックを用いても系の安定性にはあまり影響しない．
(5) 位置フィードバックを用いると系の応答が改善される．

等である．

上記の解析的方法による結論を確めるためにアナログ計算機による解析もおこなった．

1962年9月

日本原子力研究所　原子力工学部　計測制御研究室

須田　信英，三井田　純一

Contents

目　　次

Nomenclature

a Amplitude

a Ratio of sleeve temperature coefficient to moderator temperature coefficient

$C_u, C_f, C_1, C_S, C_2, C_m$ Heat capacity per unit length of channel (as for subscripts, refer to **Fig. 2.3**) cal/cm°C

$G_R(s)$ Zero power transfer function of reactor

$G_F(s)$ Temperature coefficient feedback transfer function

$G_T(s)$ Outlet gas temperature transfer function

$G_p(s)$ Overall reactor transfer function

$G_0(s)$ Overall open loop transfer function

$G_1(s)$ Transfer function defined in Eq. (3.7)

$G_2(s)$ Transfer function defined in Eq. (3.8)

$G_t(s)$ Transfer function of thermocouple

$G_{ma}(s)$ Transfer function of magnetic amplifier

$G_{mo}(s)$ Transfer function of rod drive motor

$G_N(a)$ Describing function of nonlinearity

H_1, H_2, H_3, H_4, H_5 Heat transfer coefficient per unit length along channel (As for subscripts, refer to **Fig. 2.3**) cal/cm sec°C

$K_u, K_f, K_1, K_s, K_2, K_m$ Gain constants (As for subscripts, refer to **Fig. 2.4**)

L	Core height	cm
K	Controller gain	1/sec °C
K_d	Controller gain of discontinuous control system	1/sec
K_{f1}	Tachometer feedback gain	°C sec
K_{f2}	Rod position feedback gain	°C
K_{f2c}	Threshold value of K_{f2}	°C
l	Mean effective lifetime of neutrons	sec
N	Number of revolutions	
P	Number of poles	
q	Normalized power Q/Q_0	
Q	Power per unit length along channel	cal/cm sec
R_1	Heat transfer coefficient for radiation between clad and sleeve	cal/cm sec °K^4
R_2	Heat transfer coefficient for radiation between sleeve and moderator	cal/cm sec °K^4
R_{1f}	$4T_{f0}^3R_1$	
R_{1s}	$4T_{s0}^3R_1$	
R_{2s}	$4T_{s0}^3R_2$	
R_{2m}	$4T_{m0}^3R_2$	
R_{max}	Limit of control rod speed	1/sec

s	Complex frequency	1/sec
T_I	Reset time of three action controller	sec
T_D	Rate time of three action controller	sec
T_{out}	Temperature of gas at outlet of core	°C
$T_u, T_f, T_{c1}, T_s, T_{c2}, T_m$	Temperature (As for subscripts, refer to **Fig. 2.3**)	°C
u	Velocity of gas	cm/sec
Z	Number of zeros	
α_u	Temperature coefficient of fuel	1/°C
α_s	Temperature coefficient of sleeve	1/°C
α_m	Temperature coefficient of moderator	1/°C
α_{mc}	Critical value of α_m (Refer to Eq. 2.2))	
β	Fraction of delayed neutron	
Δ	Width of deadzone	°C
λ	Decay constant of delayed neutron precursor	1/sec
μ_u, μ_s, μ_m	Proportions of power generated in fuel, sleeve and moderator, respectively	
ρ	Reactivity	
ρ_{ex}	Reactivity disturbance	
ρ_{temp}	Reactivity due to temperature change	
ρ_{rod}	Reactivity due to rod motion	
$\tau_u, \tau_f, \tau_1, \tau_s, \tau_2, \tau_m$	Time constants (As for subscripts, refer to **Fig. 2.4**)	sec
$\tau_t, \tau_{ma}, \tau_{mo}$	Time constants of thermocouple, magnetic amplifier and motor, respectively	
$\Delta T_u^*, \Delta T_s^*, \Delta T_m^*$	Zero frequency gain of $\frac{\Delta T_u(s)}{\Delta q(s)}$, $\frac{\Delta T_s(s)}{\Delta q(s)}$ and $\frac{\Delta T_m(s)}{\Delta q(s)}$, respectively	

Subscript o denotes the steady state values of variables, Δx denotes the deviation of variable x from its steady state value x_0

Parameter Values Used in Analysis

l	1.4×10^{-3}	sec
β	5.39×10^{-3}	
λ	0.0769	1/sec
a_u	-2.1×10^{-5}	1/°C
a_s	2.75×10^{-5}	1/°C
a_m	10.8×10^{-5}	1/°C
a_{mc}	2.02×10^{-5}	1/°C
C_u	5.363	cal/cm °C
C_f	3.914	cal/cm °C
C_l	0.147	cal/cm °C
C_s	23.33	cal/cm °C
C_2	0.063	cal/cm °C
C_m	234.7	cal/cm °C
R_1	2.704×10^{-11}	cal/cm sec °K^4
R_2	3.562×10^{-11}	cal/cm sec °K^4
μ_u	0.92	cal/cm sec °K^4
μ_s	0.0082	cal/cm sec °K^4
μ_m	0.0718	cal/cm sec °K^4
H_1	1.896	cal/cm sec °C
H_2	0.492	cal/cm sec °C
H_3	0.172	cal/cm sec °C
H_4	0.0233	cal/cm sec °C
H_5	0.0303	cal/cm sec °C
u_1	631	cm/sec
u_2	6.6	cm/sec
L	655	cm
Q_0	28.5	cal/cm sec
Δ	1.25	°C
τ_t	8	sec
τ_{ma}	0.2	sec
τ_{mo}	0.5	sec

1. Introduction

In British type power reactors, that is, natural uranium fueled, graphite moderated and gas cooled reactors, the temperature coefficient of the graphite moderator becomes positive as the fuel burn-up proceeds and the plutonium accumulates within the fuel.

The dynamics of this type of reactors are characterized by the positive temperature coefficient and a long thermal time constant of the core due to the large heat capacity of the graphite moderator.

If the positive temperature coefficient exceeds a certain threshold value, the reactor itself becomes unstable[1),7)]. Because of this fact the stability analysis of the control system for this type of reactors presents a unique problem for the control engineers.

Usually the controlled processes encountered in the control engineering field are stable or self-regulating, in other words, the roots of their characteristic equations are located in the left half of the complex plane. The processes with some of their characteristic roots on the imaginary axis are also often encountered. However, rarely encountered in the control system analysis are the unstable processes, which have some of their characteristic roots in the right half plane as British type power reactors do[1)].

The present work summarizes the stability analyses of such a control system by means of the generalized Nyquist's stability criterion. The describing function method is used to investigate the effects of nonlinearities involved in the system.

Some analog computer studies are also included and comparisons are made between different types of controller setup.

The numerical calculations and the analog computer runs are made using the parameter values of a reference reactor, which is similar to the JAPCO Tokai Plant at 20% load operation.

In the analysis only the reactor outlet gas temperature control system is investgated. The effect of the secondary system is not taken into consideration. The temperature coefficient feedback is considered, but the xenon poisoning effect is ignored since the change in xenon concentration is considerably slow compared to the frequency range of interest in the control system design.

The principal purpose of the present study is to determine what are the necessary conditions of stability. It is not tried to optimize the controller settings. More extensive computer studies are necessary to determine the optimum settings.

2. Description of the System Investigated

The schematic block diagram of the control system is shown in Fig. 2.1. The reactor outlet gas temperature, T_{out}, is sensed and its deviation from the set point is used to drive the control rods. The pressure in the low pressure steam line is measured and used to control the gas flow through the core and thus to match

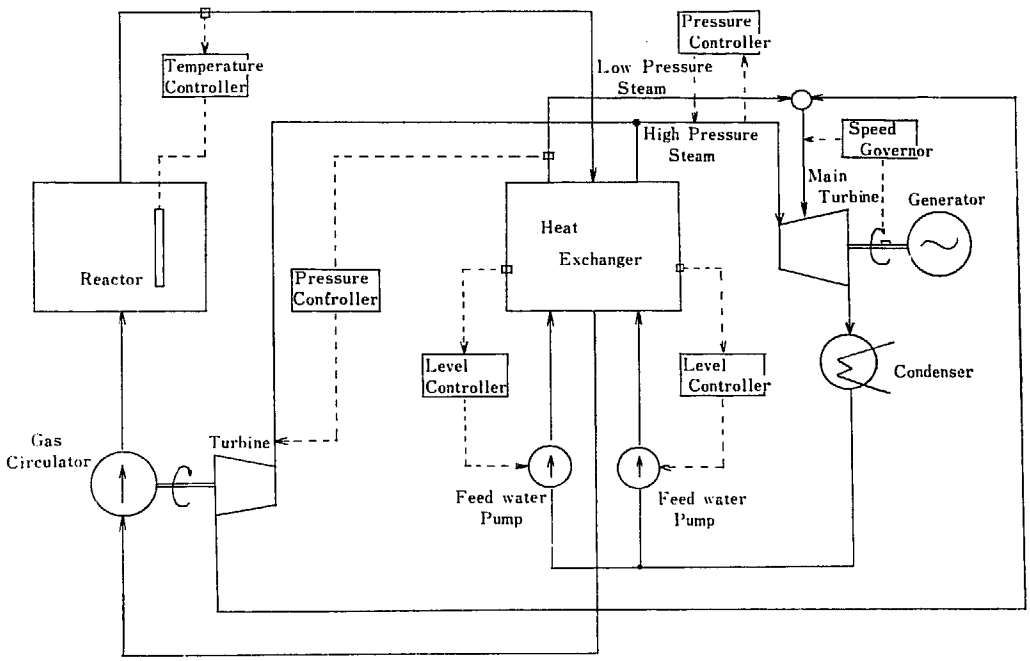

Fig. 2.1 Schematic Block Diagram of Plant Control System

the reactor power with the electrical load. Some auxiliary controllers are also included, such as drum level controllers and high pressure steam pressure regulator.

In the present report only the outlet gas temperature controller is investigated. The effect of the secondary system is not taken into consideration, that is, the flow rate and the inlet gas temperature are assumed to be constant.

In Fig. 2.2 is shown a more detailed block diagram of the outlet gas temperature control system.

The zero power transfer function $G_R(s)$ used in this analysis is a conventional, space independent, one-delayed-neutron-group approximation.

$$G_R(s)=\frac{Q_0(s+\lambda)}{ls\left(s+\frac{\beta}{l}+\lambda\right)} \tag{2.1}$$

In considering the reactor heat transfer dynamics a unit cell of the reactor core with averaged values of parameters is assumed to represent the dynamics of the whole core. Fig. 2.3 shows a cutaway view of the unit cell.

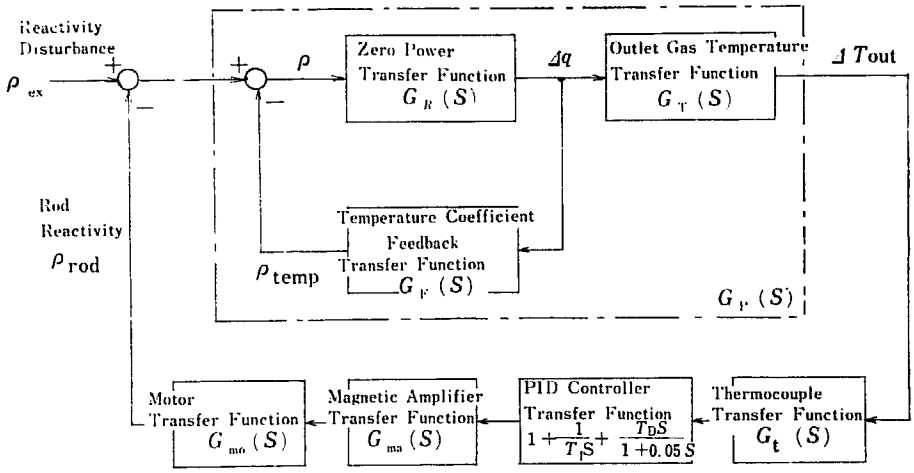

Fig. 2.2 Block Diagram of Temperature Control System

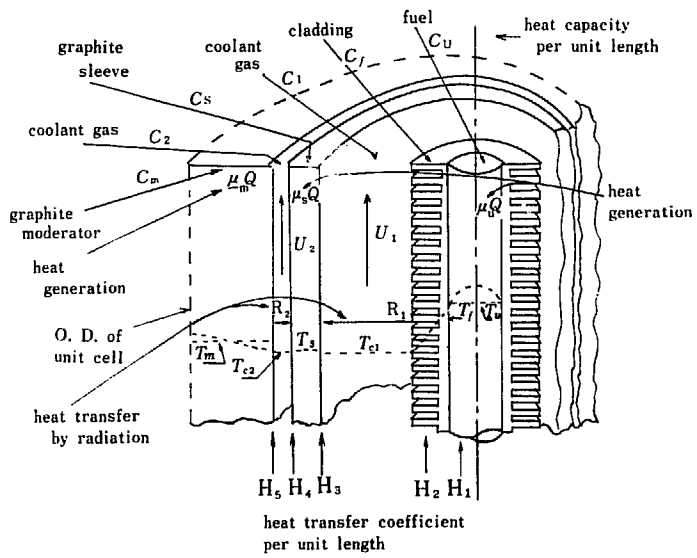

Fig. 2.3 Cutaway View of a Unit Cell

The feedback transfer function, $G_F(s)$, and the outlet gas temperature transfer function, $G_T(s)$, are obtained from the equations[1] based on the work by T. J. O'NEILL[2]. The equations are basically a lumped parameter model and it is known that they give a fairly accurate approximation to the more exact treatment of a distributed parameter model as far as the system subject to reactivity disturbance is concerned[1]. Thus the use of the lumped parameter model is adequate in this analysis, where the only disturbance to the system is a reactivity change.

The temperatures which affect the reactivity are the fuel temperature the graphite-sleeve temperature and the graphite-moderator temperature. The fuel temperature coefficient α_U is always negative, while the sleeve temperature coefficient α_S and the moderator temperature coefficient α_m become positive for high fuel burn-up.

The block diagram of the reactor heat transfer dynamics thus obtained is shown in **Fig. 2.4**, from which $G_F(s)$ and $G_T(s)$ are obtained.

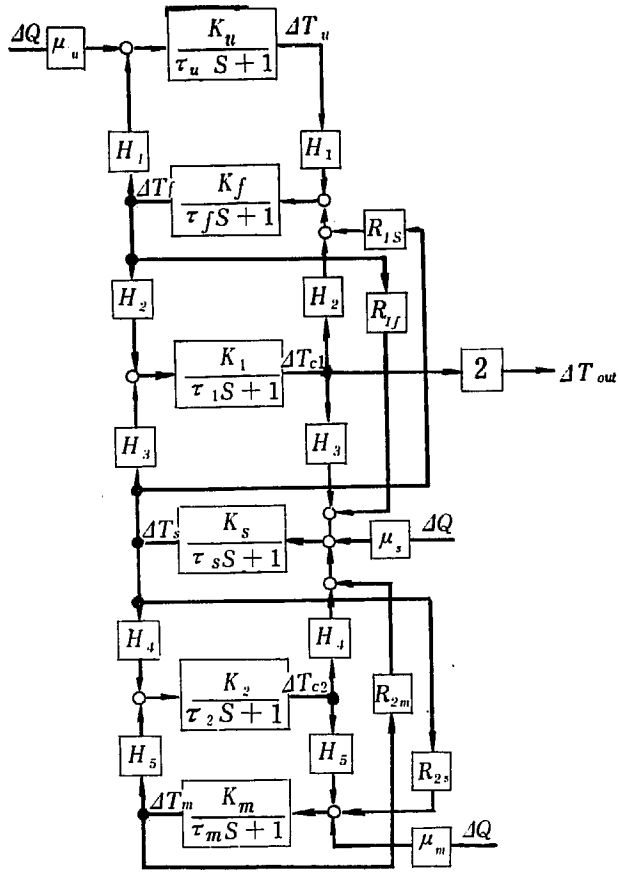

$$\tau_U = \frac{C_U}{H_1} \qquad K_U = \frac{1}{H_1}$$

$$\tau_f = \frac{C_f}{H_1+H_2+R_{1f}} \qquad K_f = \frac{1}{H_1+H_2+R_{1f}}$$

$$\tau_1 = \frac{C_1}{H_2+H_3+\frac{2C_1u_1}{L}} \qquad K_1 = \frac{1}{H_2+H_3+\frac{2C_1u_1}{L}}$$

$$\tau_s = \frac{C_s}{H_4+H_3+R_{1s}+R_{2s}} \qquad K_s = \frac{1}{H_4+H_3+R_{1s}+R_{2s}}$$

$$\tau_2 = \frac{C_2}{H_4+H_5+\frac{2C_2u_2}{L}} \qquad K_2 = \frac{1}{H_4+H_5+\frac{2C_2u_2}{L}}$$

$$\tau_m = \frac{C_m}{H_5+R_{2m}} \qquad K_m = \frac{1}{H_5+R_{2m}}$$

Fig. 2.4 Block Diagram for Reactor Thermal System

The analytical forms of $G_F(s)$ and $G_T(s)$ are so involved that their frequency responses are calculated by an analog computer.

Now the zero power transfer function modified by $G_F(s)$ and $G_T(s)$ forms the "overall" transfer function $G_P(s)$ of the reactor, that is,

$$G_P(s) = \frac{G_R(s)G_T(s)}{1+G_R(s)G_F(s)} \tag{2.2}$$

Since $G_P(s)$ includes an internal feedback path, the stability of this minor feedback loop should be determined first. It is shown in Ref.1) that this loop is unstable if

a_m satisfies the following condition:

$$a_m > a_{mc} = \frac{-a_u \Delta T_u^*}{a \Delta T_s^* + \Delta T_m^*} \tag{2.3}$$

where the ratio $a = a_s/a_m$ is assumed to be constant and independent of burn-up.

The vector loci of the open loop transfer function $G_R(s) \cdot G_F(s)$ are shown in **Fig. 2.5** both for $a_m > a_{mc}$ and $a_m < a_{mc}$. Application of the Nyquist's criterion reveals that if $a_m > a_{mc}$, the characteristic equation

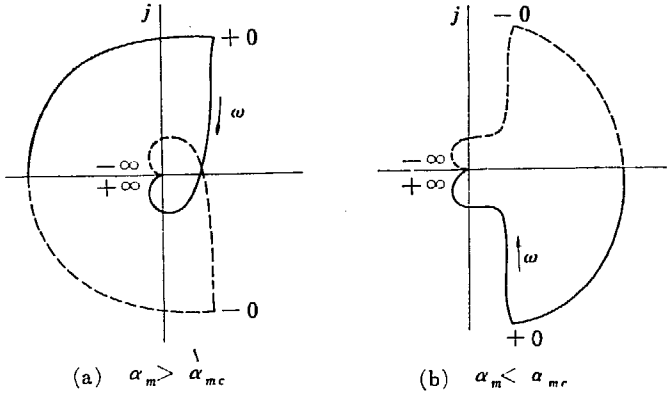

Fig. 2.5 Vector Locus of $G_R(j\omega)G_F(j\omega)$

$$1 + G_R(s) \cdot G_F(s) = 0 \tag{2.4}$$

has one root in the right half plane, namely, the $G_p(s)$ given by Eq. (2.2) has one pole in the right half plane. If $a_m < a_{mc}$, $G_p(s)$ has no pole in the right half plane. This fact indicates that $G_P(s)$ is an unstable system for $a_m > a_{mc}$ and a stable one for $a_m < a_{mc}$, as are expected.

The moderator temperature coefficient a_m of the reference reactor is about 1.08×10^{-4}/°C, while a_{mc} for the same reactor is 2.02×10^{-5}/°C. Thus the reactor is essentially unstable and its transfer function has one pole in the right half plane.

Substituting the numerical values into Eq. (2.2) the overall reactor transfer function $G_p(s)$ is obtained. The results are shown in the Bode's charts in **Fig. 2.6.**

The transfer function of the controller is simplified as shown in **Fig. 2.2.** It basically consists of the time lag of the thermocouple, the proportional, reset and rate actions, the lag of the magnetic amplifier and the transfer function of the rod drive motor. These transfer functions are assumed as follows:

$$G_t(s) = \frac{1}{1 + \tau_t s} \tag{2.5}$$

$$G_{ma}(s) = \frac{1}{1 + \tau_{ma} s} \tag{2.6}$$

$$G_{mo}(s) = \frac{K}{s(1 + \tau_{mo} s)} \tag{2.7}$$

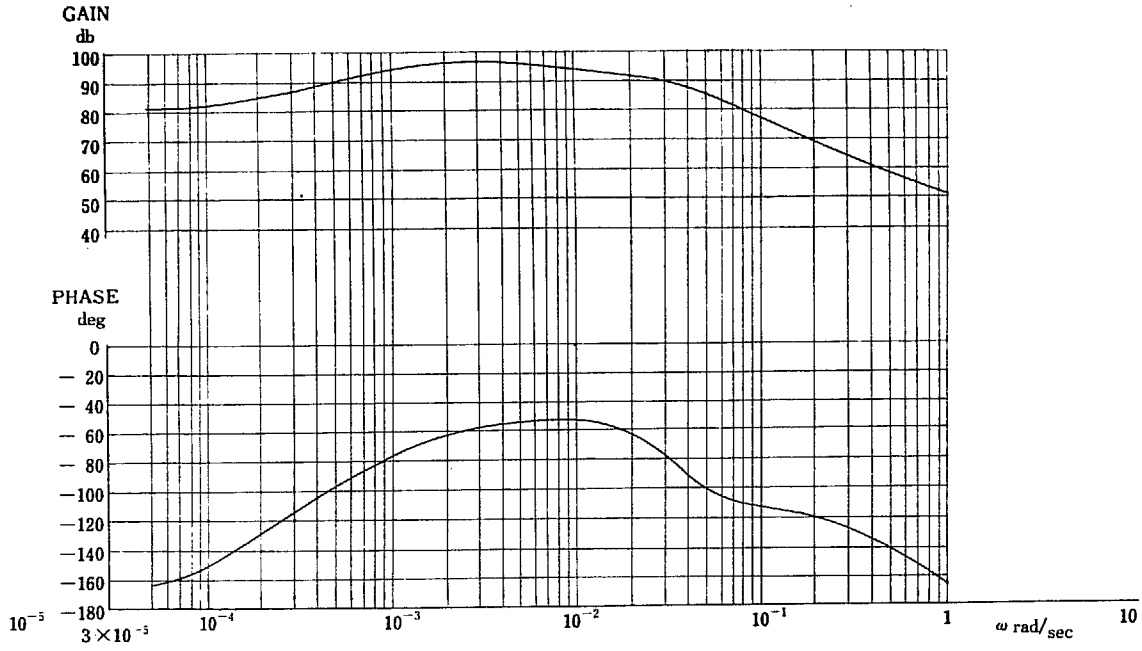

Fig. 2.6 Bode's Charts for $G_p(j\omega)$

Some modifications are made to this basic system as described below.

In the first section of the next chapter an analysis is made on the stability of the basic continuous control system shown in Fig. 2.2. The transfer function of the controller for this case is shown in Fig. 2.7 (a).

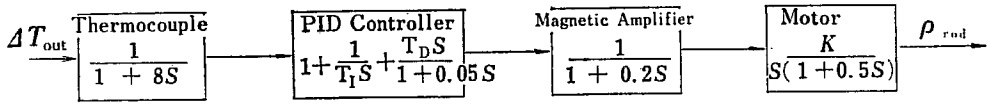

Fig. 2.7 (a) Block Diagram of Controller for Basic System

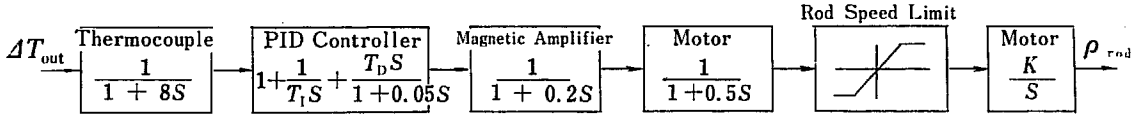

Fig. 2.7 (b) Block Diagram of Controller for Continuous Control with Rod Speed Saturation

In the actual system there is always some deadzone or saturation due to imperfection of the equipment. In some cases such nonlinearities are introduced artificially. For example, the saturation in the control rod speed is necessary from safety considerations. The deadzone is effective to avoid rapid wear of the equipment due to noise in the system. Therefore an analysis is made, in Sec. 3.2, on the effects of saturation and deadzone on both the stability and indicial responses of the system.

In Sec. 3.3, an analysis of the discontinuous control system is presented. The block diagram of the discontinuous controller is shown in Fig. 2.7 (c). The describing function method first developed by R. J. Kochenburger[3] was used to determine the

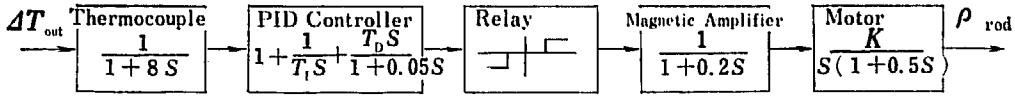

Fig. 2.7 (c) Block Diagram of Controller for Discontinuous Control System

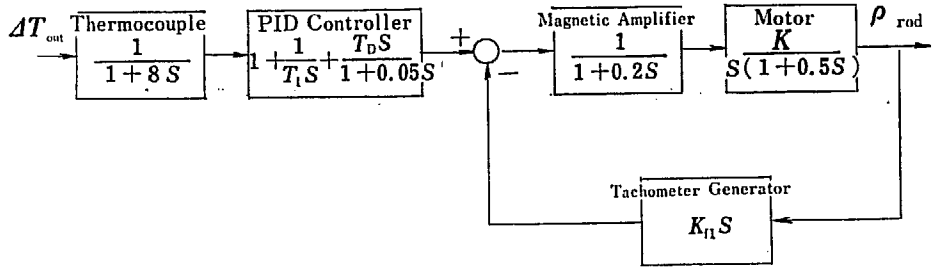

Fig. 2.7 (d) Block Diagram of Controller for Continuous Control with Tachometer Feedback

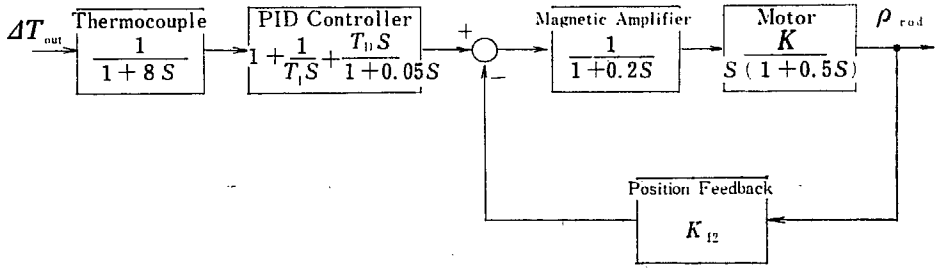

Fig. 2.7 (e) Block Diagram of Controller for Continuous Control with Position Feedback

stability of this system.

A modified system with tachometer feedback, shown in Fig. 2.7 (d) is analyzed in Sec. 3.4.

Finally, a modified system with the rod position feedback, shown in Fig. 2.7 (e), is analyzed in Sec. 3.5.

3. Stability Analysis

3.1 Continuous Control*

The overall open loop transfer function of the continuous control system is easily obtained from Fig. 2.2 and Fig. 2.7 (a),

$$KG_0(s)=G_P(s)\frac{1}{1+8s}\left(1+\frac{1}{T_{Is}}+\frac{T_{Ds}}{1+0.05s}\right)\frac{1}{1+0.2s}\frac{1}{1+0.5s}\frac{K}{s} \qquad (3.1)$$

The vector locus of $KG_0(s)$ is shown in Fig. 3.1. In Fig. 3.1 (a) is shown the locus for $a_m>a_{mc}$, which is the case for the reference reactor. In Fig. 3.1 (b), the locus for $a_m<a_{mc}$ is shown for the purpose of comparison.

Now the generalized Nyquist's criterion[4] states that the system is stable, if and only if Z, given by the following equation, is equal to zero,

* Sections 3.1 through 3.3 are included for completeness' sake, although major part of their contents has already been published elsewhere.[5]

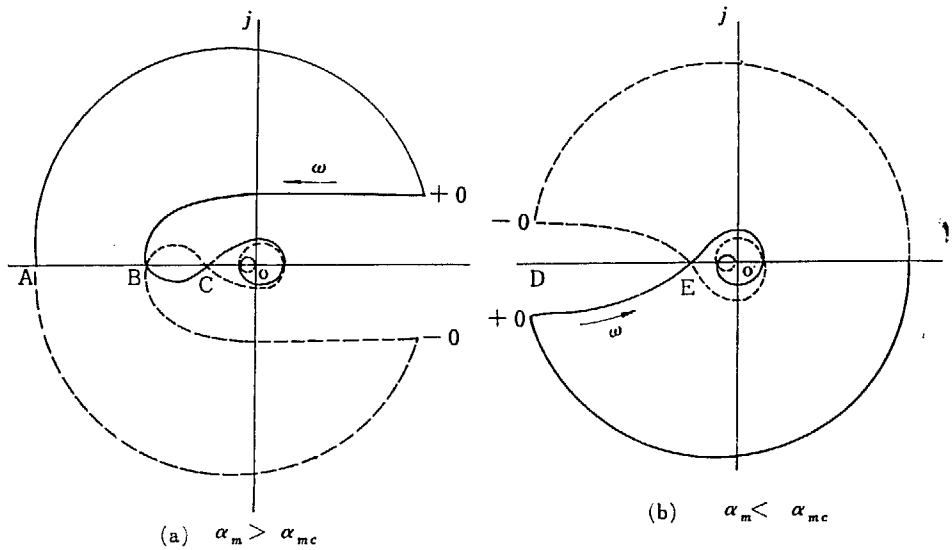

Fig. 3.1 Vector Locus of $G_0(j\omega)$

$$Z=N+P \tag{3.2}$$

where N is the number of clockwise revolutions of the $KG_0(s)$ locus around $(-1, 0)$ when s traverses from $-j\infty$ to $j\infty$ along the imaginary axis of the s plane and then around a semicircular path of an infinite radius enclosing the right half of the s plane, P is the number of poles of $KG_0(s)$ with positive real parts, and Z is the number of roots of $KG_0(s)=-1$ with positive real parts.

It is shown in Chapt. 2 that $KG_0(s)$ has one pole with positive real part if $\alpha_m > \alpha_{mc}$, that is $P=1$ in this case. Therefore the system is stable, if and only if $N=-1$. **Fig. 3.1** (a) shows that $N=1$ if the point $(-1, 0)$ is on the segment AB of the real axis, $N=-1$ if it is on the segment BC and N is greater than 1 if it is on the segment CO. Therefore the system is stable only if the point $(-1, 0)$ lies on the segment BC, which means that the system is unstable if the gain is either too high or too low. The low gain instability is due to the divergent tendency of the controlled process. If the controller gain is too low, it cannot suppress the divergent tendency and the system undergoes a divergent oscillation. The high gain instability is quite common in various control systems.

If $\alpha_m < \alpha_{mc}$, P is obviously zero and the system is stable if the point $(-1, 0)$ is on the segment DE of **Fig. 3.1** (b). Accordingly the system becomes unstable if the gain is too high but it is stable no matter how low the gain is, as is expected.

Substituting the numerical values, the Bode's Charts of $KG_0(s)$ are obtained for several different combinations of the controller parameters T_I and T_D, which are shown in **Fig. 3.2.** From this chart the limits of the gain and the frequency of sustained oscillation at these limits are obtained as shown in **Table 3.1.** The values obtained from the analog computer study are shown in the brackets. The agreement of the two results is quite satisfactory.

It is noted from **Fig. 3.2,** that the low frequency portion of the frequency response

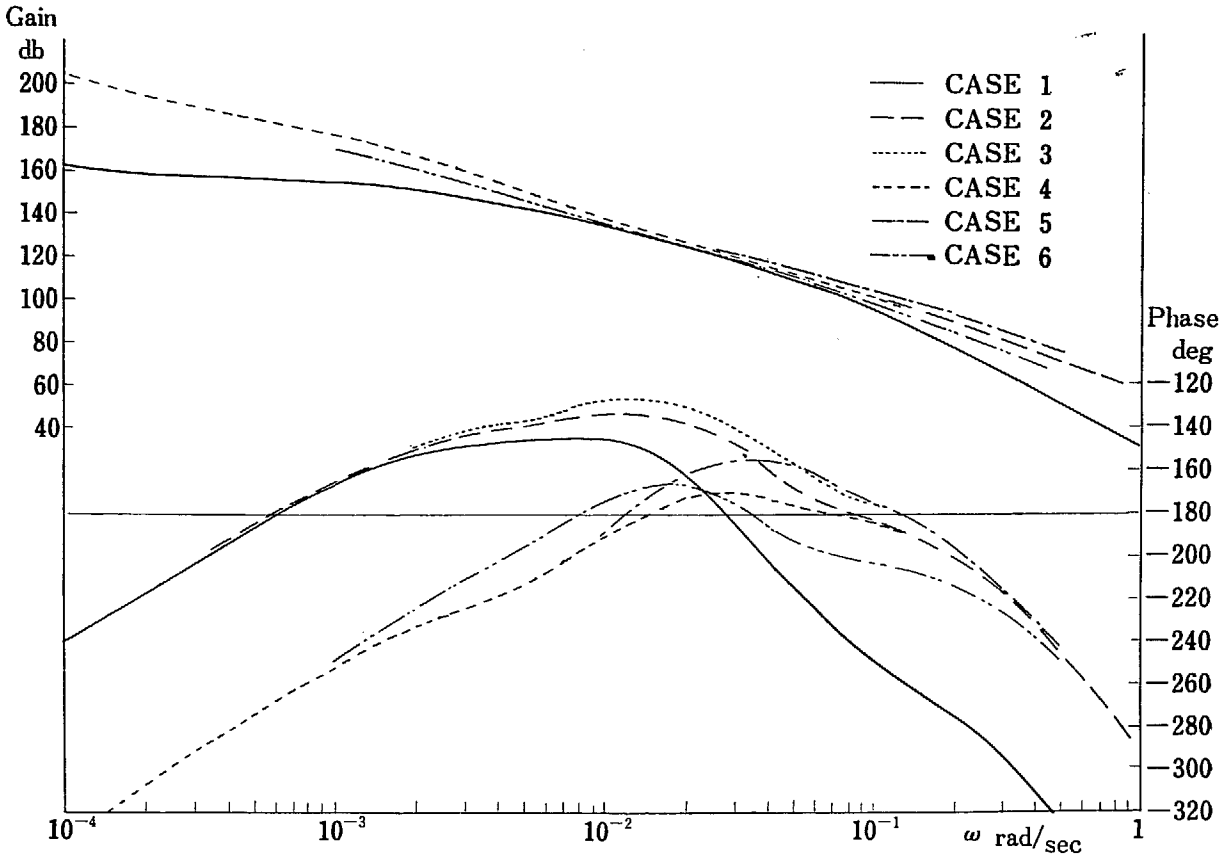

Fig. 3.2 Bode's Charts for $G_0(j\omega)$

Table 3.1. Stability Limits for Continuous Control

Case No.	T_I sec	T_D sec	Upper Limit of Gain 10^{-5}/sec °C	Frequency of Oscillation rad/sec	Lower Limit of Gain 10^{-5}/sec °C	Frequency of Oscillation rad/sec
1	∞	0	0.112	0.028	0.0016	0.00062
2	∞	20	0.64	0.094	0.0016	0.0006
3	∞	30	1.0 (1.0)	0.125 (0.128)	0.0016	0.0006
4	80	20	0.448 (0.46)	0.068 (0.069)	0.032 (0.032)	0.015 (0.0146)
5	80	30	1.0 (1.0)	0.125 (0.126)	0.0224 (0.025)	0.0122 (0.0125)
6	160	10	0.144 (0.128)	0.034 (0.035)	0.0144	0.0082

Values in brackets are those obtained by analog computer

is primarily dependent on T_I while the high frequency portion is mainly influenced by T_D.

With proportional action only (Case 1), the system has a considerable stable region. The upper and lower limits are about 35 db apart. Introduction of rate action (Case 2 and 3) improves the system stability. The stable region is now more than 2 decades. If reset action is added (Cases 4, 5 and 6), the system becomes less stable. These conclusions are confirmed by the analog computer studies in Chapt. 4.

3.2 Effects of Controller Nonlinearities

The effects of the controller nonlinearities on the system stability are investigated by means of the Kochenburger's describing function technique[3].

The describing functions $G_N(a)$ of the saturation and the deadzone are shown in **Fig. 3.3.** The locus of inverse describing function $-1/G_N(a)$ is plotted together with the locus of $KG_0(s)$ in **Fig. 3.4.** Applied to **Fig. 3.4.**, the Kochenburger's theorem gives the following conclusions.

(i) Deadzone

If the point (−1, 0) is on the segment AB, the system diverges.

If it is on the segment BC, the system converges to a stable limit cycle L_1,

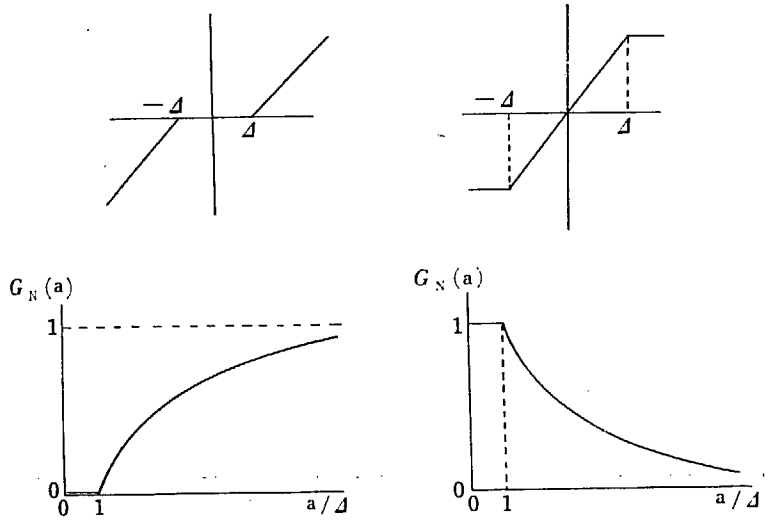

(a) Deadzone and its Describing Function

(b) Saturation and its Describing Function

Fig. 3.3 Nonlinearities and Their Describing Functions

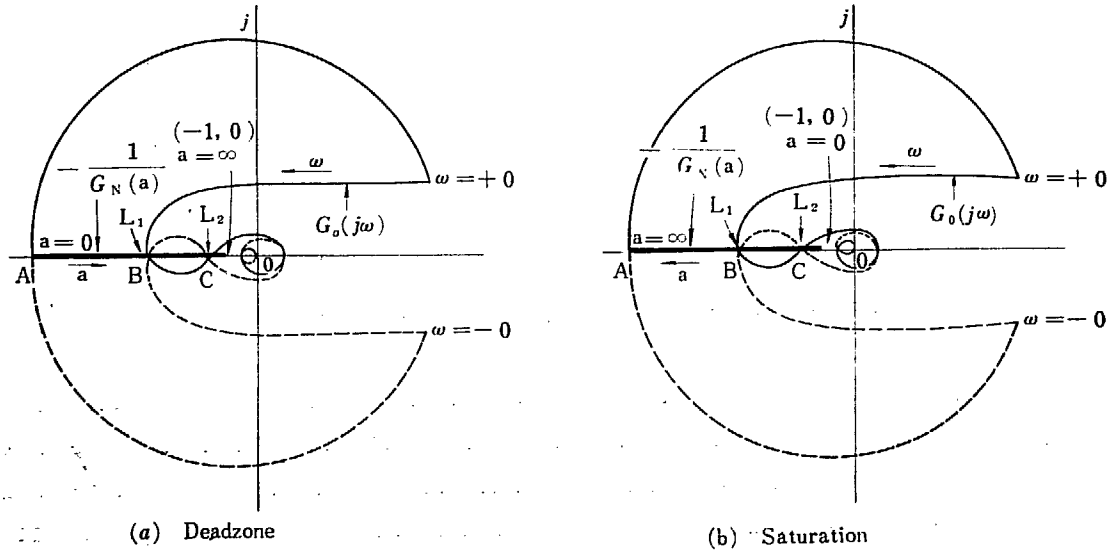

(a) Deadzone

(b) Saturation

Fig. 3.4 Vector Loci of $G_0(j\omega)$ and $-1/G_N(a)$

whatever the initial amplitude may be.

If it is on the segment CO, there exist two limit cycles; a stable one L_1 and an unstable one L_2. If the initial amplitude is smaller than L_2, the system converges to the limit cycle L_1; if not, the system diverges.

(ii) Saturation

If the point (−1, 0) is on the segment AB, the system diverges.

If it is on the segment BC, there exists an unstable limit cycle L_1. If the initial amplitude is smaller than L_1, the system is stable and finally the amplitude becomes zero; if not, the system diverges.

If the point (−1, 0) is on the segment CO, there exist two limit cycles; an unstable one L_1 and a stable one L_2. If the initial amplitude is smaller than L_1, the system converges to L_2; if not, the system diverges.

Thus, the conclusions are as follows; if the system contains saturation, the system is not controllable and diverges for a very large disturbance at any choice of gain and, if it contains deadzone, it is possible to design the system in such a way that it does not diverge although the limit cycle is inevitable.

3.3 Discontinuous Control

In studying the stability of the discontinuous control system, the characteristics of the relay is assumed to have a deadzone but not hysteresis as shown in **Fig. 3.5.** The describing function of such a relay is also shown in **Fig. 3.5**, the reciprocal of

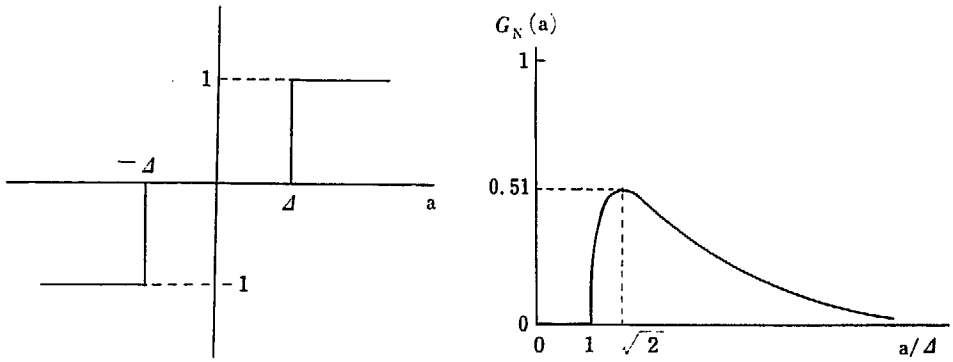

Fig. 3.5 Relay Characteristics and Relay Describing Function

which is plotted in **Fig. 3.6** together with $KG_0(s)$. The locus of $-1/G_N(a)$ starts from $-\infty$ on the real axis and moves towards the origin as a increases. The distance from the origin is smallest for $a=\sqrt{2}\Delta$, that is $-1/G_N(a)=-1.96$. The locus turns back for larger value of a and again tends to $-\infty$ as $a\to\infty$. Thus the point (−1.96, 0) is the critical point of stability analysis instead of (−1, 0) in the previous sections. And the system stability depends upon the location of this point as described below.

(i) The point (−1.96, 0) is on the segment AB

——The system diverges.

(ii) The point (−1.96, 0) is on the segment BC

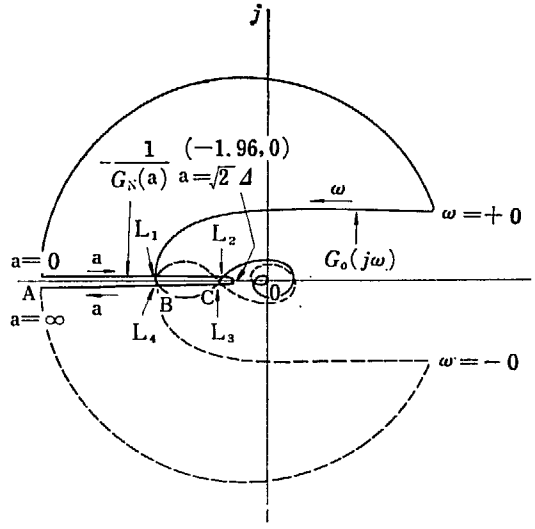

Fig. 3.6 Vector Loci of $G_0(j\omega)$ and $-1/G_N(a)$ for Discontinuous Control System

——There exist two limit cycles; a stable one L_1 and an unstable one L_4. If the initial amplitude is smaller than L_4, the system converges to L_1; if not, the system diverges.

(iii) The point (−1.96, 0) is on the segment CO

——There exist four limit cycles; two stable ones L_1 and L_3 and two unstable ones L_2 and L_4. If the initial amplitude is smaller than L_2, the system converges to L_1. If the initial amplitude is between L_2 and L_4, the system converges to L_3. If the initial amplitude is larger than L_4, the system diverges.

Thus, in case of the discontinuous controller, the limit cycle is inevitable whatever the system gain may be and the system diverges if the disturbance is larger than a threshold value.

Assuming the controller parameters of Case 5 (T_I=80 sec, T_D=30 sec), some quantitative analysis of the discontinuous control system are made. The deadzone width Δ is assumed to be $1\frac{1}{4}$ °C.

The critical gains at which the transition from Case (i) to Case (ii) and from Case (ii) to Case (iii) occur are obtained from the value of $G_N(\sqrt{2}\,\Delta)$ and the system gains at points B and C as below.

The boundary of Case (i) and Case (ii) K_d*$=4.5\times10^{-7}$/sec.

The boundary of Case (ii) and Case (iii) $K_d=2\times10^{-5}$/sec.

The latter boundary is also obtained by an analog computer. The value by analog computer is $K_d=1.4\times10^{-5}$/sec and is quite close to the value obtained by Kochenburger's method.

More detailed analyses are presented in Chapt. 4 of the limit cycles and the threshold of the disturbance.

---

* The controller gain of the discontinuous control, K_d, is distinguished from that of the continuous control K, the dimension of K_d is the reactivity per unit time, while that of K is the reactivity per unit time and per unit temperature change.

3.4 Continuous Control with Tachometer Feedback

The block diagram of the controller is shown **Fig. 2.7 (d)**. It is readily seen from this diagram that the open loop transfer function of the whole system is given by

$$KG_0(s)=G_p(s)\frac{1}{1+8s}\left(1+\frac{1}{T_{IS}}+\frac{T_{DS}}{1+0.05s}\right)\frac{K}{(1+0.5s)(1+0.2s)+KK_{f1}}\frac{1}{s} \tag{3.3}$$

which can be rewritten as

$$KG_0(s)=G_p(s)\frac{1}{1+8s}\left(1+\frac{1}{T_{IS}}+\frac{T_{DS}}{1+0.05s}\right)\frac{K'}{(1+\tau_1 s)(1+\tau_2 s)}\frac{1}{s} \tag{3.4}$$

where

$$\left.\begin{aligned} K'&=\frac{K}{1+KK_{f1}}\\ \tau_1+\tau_2&=\frac{0.5+0.2}{1+KK_{f1}}\\ \tau_1\tau_2&=\frac{0.5\times 0.2}{1+KK_{f1}}\end{aligned}\right\} \tag{3.5}$$

Comparison of Eq. (3.4) with Eq. (3.1) for the basic continuous control reveals that the effect of tachometer feedback is to reduce the effective system gain by a factor of $1/(1+KK_{f1})$ and to change the controller time constants from 0.2 and 0.5 sec. to τ_1 and τ_2. Therefore the same conclusions as those given in Sec. 3.1 are also valid for this system, except the numerical values of the parameters. No further discussion is made on this system.

3.5 Continuous Control with Rod Position Feedback

The block diagram of the controller is shown in **Fig. 2.7 (e)**. The overall open loop transfer function in this case is given by

$$KG_0(s)=G_p(s)\frac{1}{1+8s}\left(1+\frac{1}{T_{IS}}+\frac{T_{DS}}{1+0.05s}\right)\frac{K}{s(1+0.5s)(1+0.2s)+KK_{f2}} \tag{3.6}$$

Compared to Eq. (3.1), it is noted that the $1/s$ term in the controller transfer function is eliminated. This is one of the principal differences between the basic system and the system considered here as is described in Chapt. 4.

Combined with the reactor transfer function, the block diagram of the whole system is given by **Fig. 3.7**, where $G_1(s)$ and $G_2(s)$ represent the following transfer functions.

$$G_1(s)=G_p(s)\frac{1}{1+8s}\left(1+\frac{1}{T_{IS}}+\frac{T_{DS}}{1+0.05s}\right) \tag{3.7}$$

$$G_2(s)=\frac{1}{1+0.2s}\,\frac{1}{1+0.5s}\,\frac{1}{s} \tag{3.8}$$

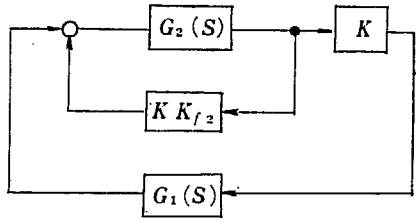

Fig. 3.7 Simplified System Diagram for Continuous Control with Rod Position Feedback

The characteristic equation of this system is given by

$$1+G_1\frac{KG_2}{1+KK_{f2}G_2}=0 \tag{3•9}$$

which is equivalent to

$$1+KK_{f2}G_2+KG_1G_2=0 \tag{3•10}$$

In order to obtain conditions of stability, the vector locus of the transfer function

$$G(s)=KG_2(s)\{K_{f2}+G_1(s)\} \tag{3•11}$$

is examined. The vector locus of $G_1(s)$ is shown in **Fig. 3.8.** According to the magnitude of K_{f2}, the locus of $\{K_{f2}+G_1(s)\}$ is divided into two types, namely, the

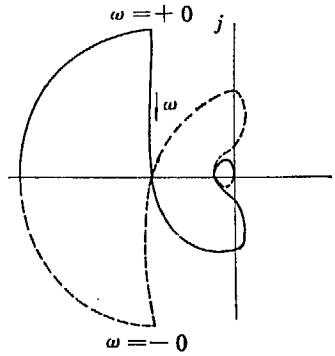

Fig. 3.8 Vector Locus of $G_1(j\omega)$

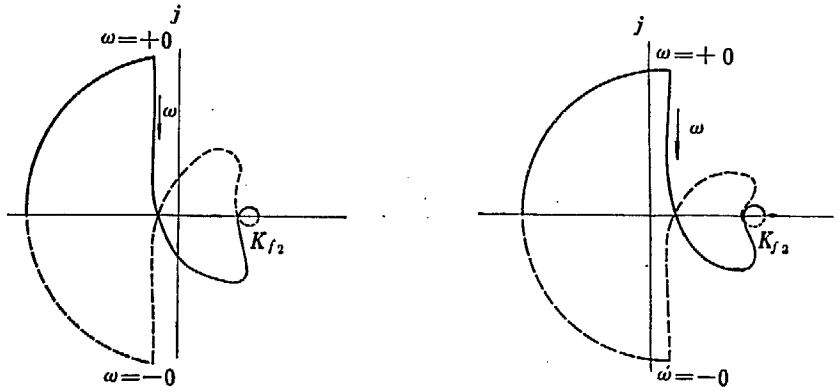

(A) $K_{f2}<K_{f2c}$ (B) $K_{f2}>K_{f2c}$

Fig. 3.9 Vector Locus of $(K_{f2}+G_1)$

one shown in Fig. 3.9 (a) and the one in Fig. 3.9 (b). The locus of $G(s)$ is shown in Fig. 3.10 (a) for the first type and in Fig. 3.10 (b) for the second type, respectively. Since $|G_1(j\omega)|$ attenuates very rapidly for large values of ω, the locus of $G(j\omega)$ approaches to that of $KK_{f2}G_2$ as ω increases, in both cases. Now the generalized Nyquist's criterion is applied to the loci of Fig. 3.10 and the following conclusions are obtained.

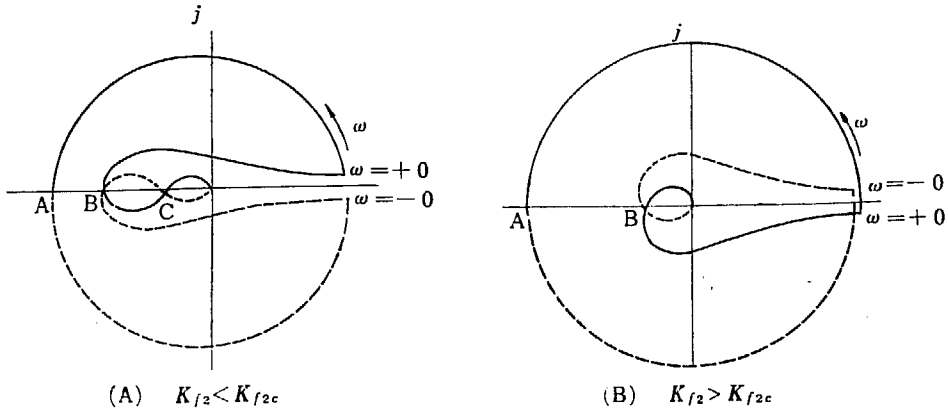

Fig. 3.10 Vector Locus of $G=KG_2(K_{f2}+G_1)$

(i) Small K_{f2} (Fig. 3.10 (a))

If the point $(-1, 0)$ is on the segment AB, $N=1$. Thus the system is unstable.

If it is on the segment BC, $N=-1$, Thus the system is stable.

If it is on the segment CO, $N=1$. Thus the system is unstable.

(ii) Large K_{f2} (Fig. 3.10 (b))

If the point $(-1, 0)$ is on the segment AB, $N=1$. Thus the system is unstable.

If it is on the segment BO, $N=2$. Thus the system is again unstable.

Therefore it is noticed that if the feedback gain K_{f2} exceeds a certain threshold value, say K_{f2c}, the system is unstable. If K_{f2} is smaller than K_{f2c}, the conditions of stability are, qualitatively at least, the same as those given in Sec. 3.1.

The Bode's charts for $G_1(j\omega)$ are shown in Fig. 3.11, for two sets of values of the controller parameters, that is

$$\begin{cases} T_I = 80 \text{ sec} \\ T_D = 30 \text{ sec} \end{cases}$$

and

$$\begin{cases} T_I = 80 \text{ sec} \\ T_D = 20 \text{ sec} \end{cases}$$

From Fig. 3.11 the value of K_{f2c} is readily obtained to be 117 db.

The overall open loop transfer function $G(s)$ is shown in the Bode's charts of Fig. 3.12 for several different values of K_{f2}. The function $G_2(s)$ is shown by the dashed line, for comparison. There are no significant differences between the curves for

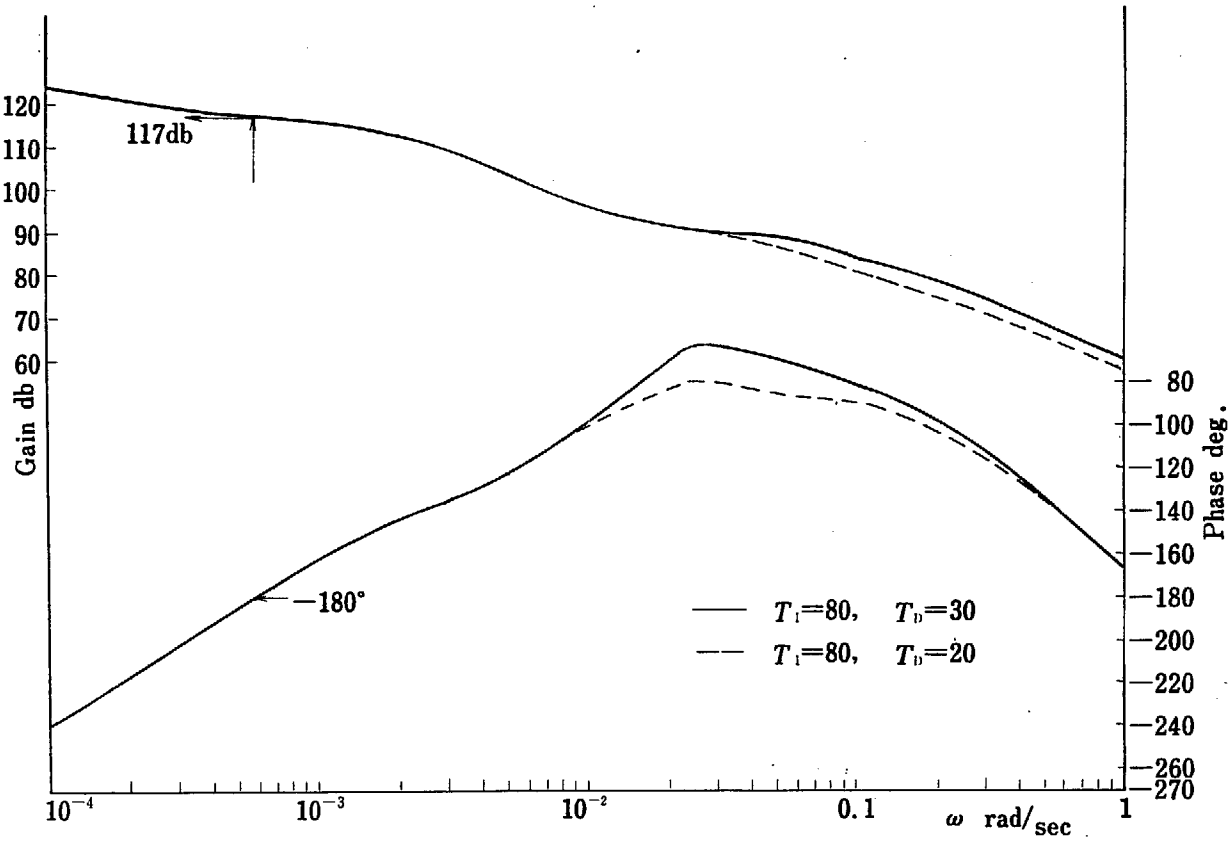

Fig. 3.11 Bode's Charts for $G_1(j\omega)$

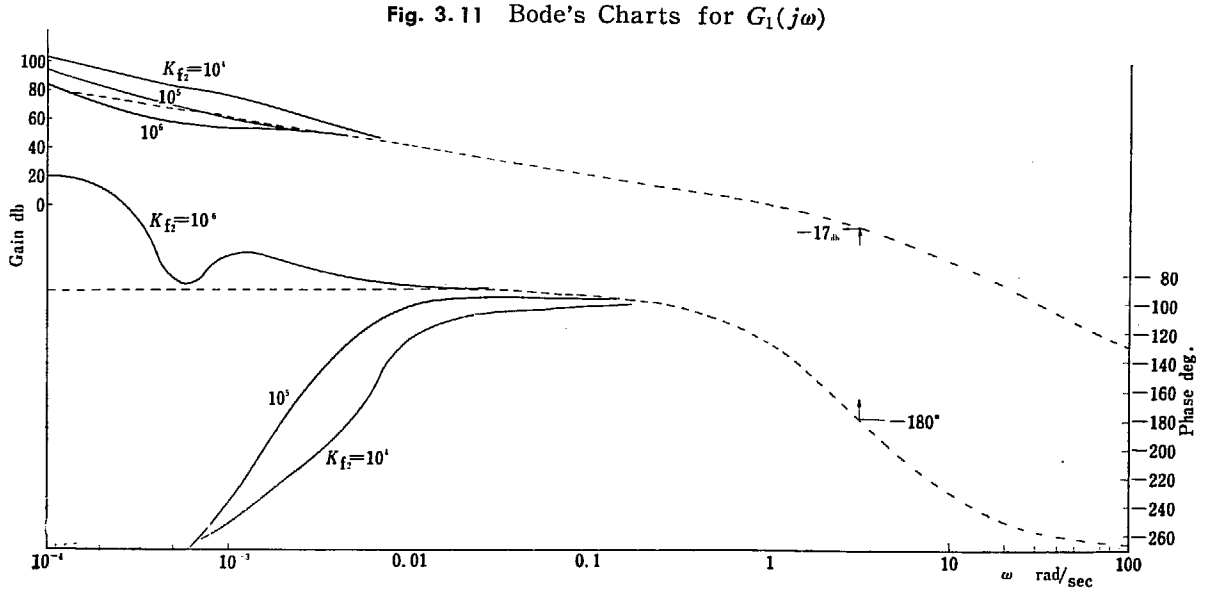

Fig. 3.12 Bode's Charts for $G(j\omega)/K_{f2}K$

T_I=80, T_D=30 and those for T_I=80, T_D=20. At high frequencies the function $G(s)/KK_{f2}$ approaches to $G_2(s)$.

It is noticed that there is no stable region for the case of $K_{f2}=10^6=120$ db, as is expected from the fact $K_{f2}>K_{f2e}$. The stable regions for other values of K_{f2} are given in Table 3.2 and are compared with those for $K_{f2}=0$ obtained in Sec. 3.1. The

Table 3.2 Stability Limits for Different Values of K_{f2}

T_I sec	T_D sec	K_{f2} °C	Upper Limit of Gain 10^{-5}/sec °C	Frequency of Oscillation rad/sec	Lower Limit of Gain 10^{-5}/sec °C	Frequency of Oscillation rad/sec
80	20 30	10^5	7.1	3.2	0.00225	0.002
80	20 30	10^4	71	3.2	0.0282	0.005
80	20	0	0.448	0.068	0.032	0.015
80	30	0	1.0	0.125	0.0224	0.0122

comparison reveals the following conclusions:

(1) The frequency of the upper limit of stability, ω_1, is much higher for the system with position feedback than for the basic system.

(2) The upper limit for the system with position feedback is given by $KK_{f2}=-17$ db, as is shown in Fig. 3.12. Therefore K_{max} is inversely propotional to K_{f2} and the frequency ω_1 is independent of K_{f2}.

(3) The lower limit K_{min} decreases as K_{f2} increases.

(4) The frequency of the lower limit of stability, ω_2, is much smaller for the system with position feedback.

(5) The ratio of K_{max} and K_{min} which determines the magnitude of stable region, is about 10 times as large as that of the basic system.

The above conclusions suggest that the system discribed here is better than basic system, from the viewpoint of the system stability. More detailed analyses and comparisons are presented in Chapt. 4.

4. Analog Computer Studies

Some analog computer studies are made in order to verify the results of the analyses presented in the preceding chapter and to estimate the magnitude of transient temperature rise.

4.1 Basic Continuous Control

4.1.1 Stability Limits

The stability limits for different controller settings are examined. The results are shown in Table 3.1. They show good agreement with the results by the analytical method.

Examples of stable and unstable responses are shown in Figs. 4.1 and 4.2. Three typical responses of Case 5 are shown in Fig. 4.1. Fig. 4.1 (a) is unstable because the gain is too high and Fig. 4.1 (c) is also unstable because the gain is too low. Fig. 4.1 (b) shows an example of stable responses. Typical responses of Case 3 for several different controller gain are shown in Fig. 4.2.

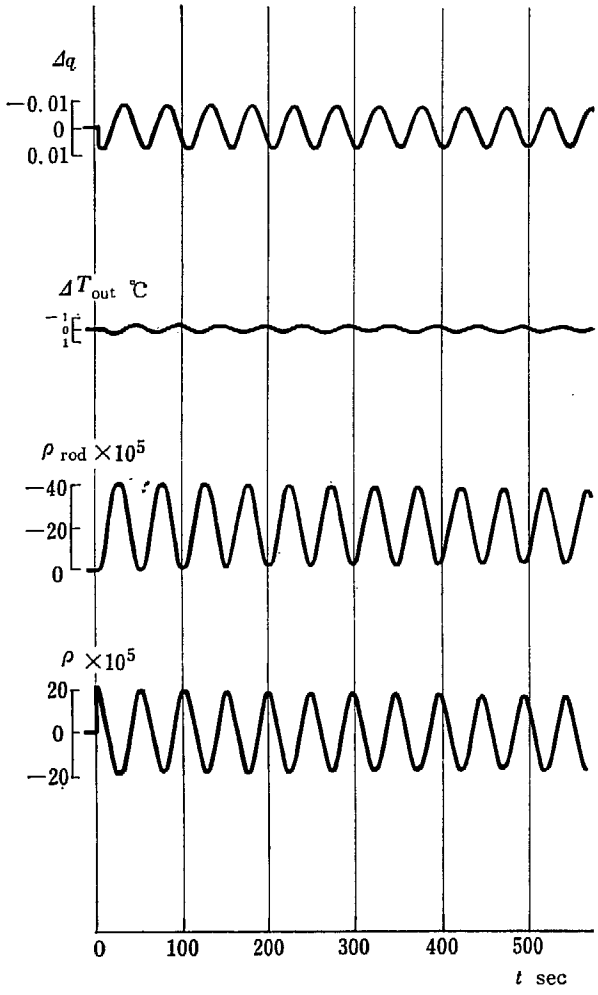

Fig. 4.1 (a) Examples of Transient Responses
$K=10^{-5}$/sec °C
$T_I=80$ sec $T_D=30$ sec $\rho_{ex}=2\times10^{-4}$

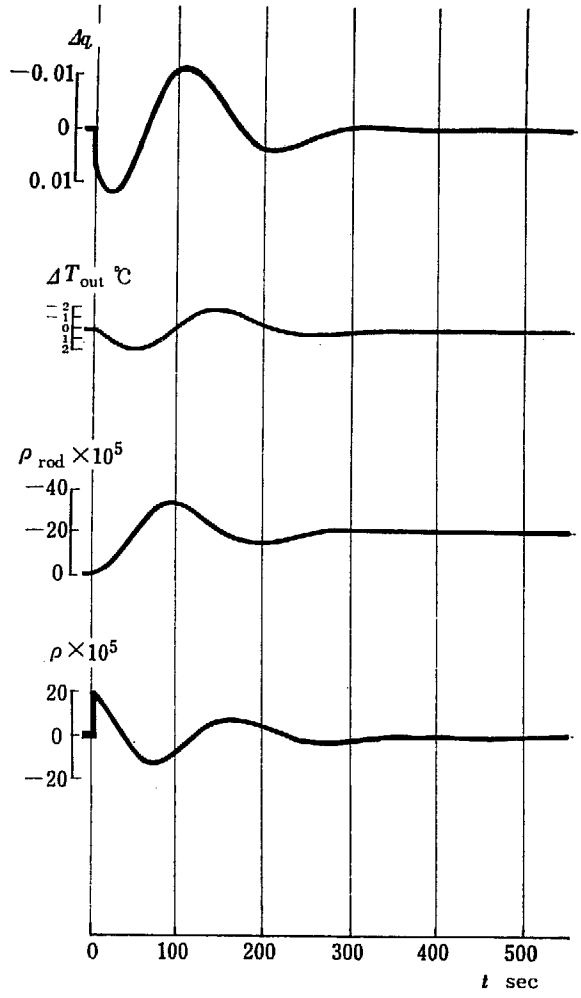

Fig. 4.1 (b) Examples of Transient Responses
$K=0.1\times10^{-5}$/sec °C
$T_I=80$ sec $T_D=30$ sec $\rho_{ex}=2\times10^{-4}$

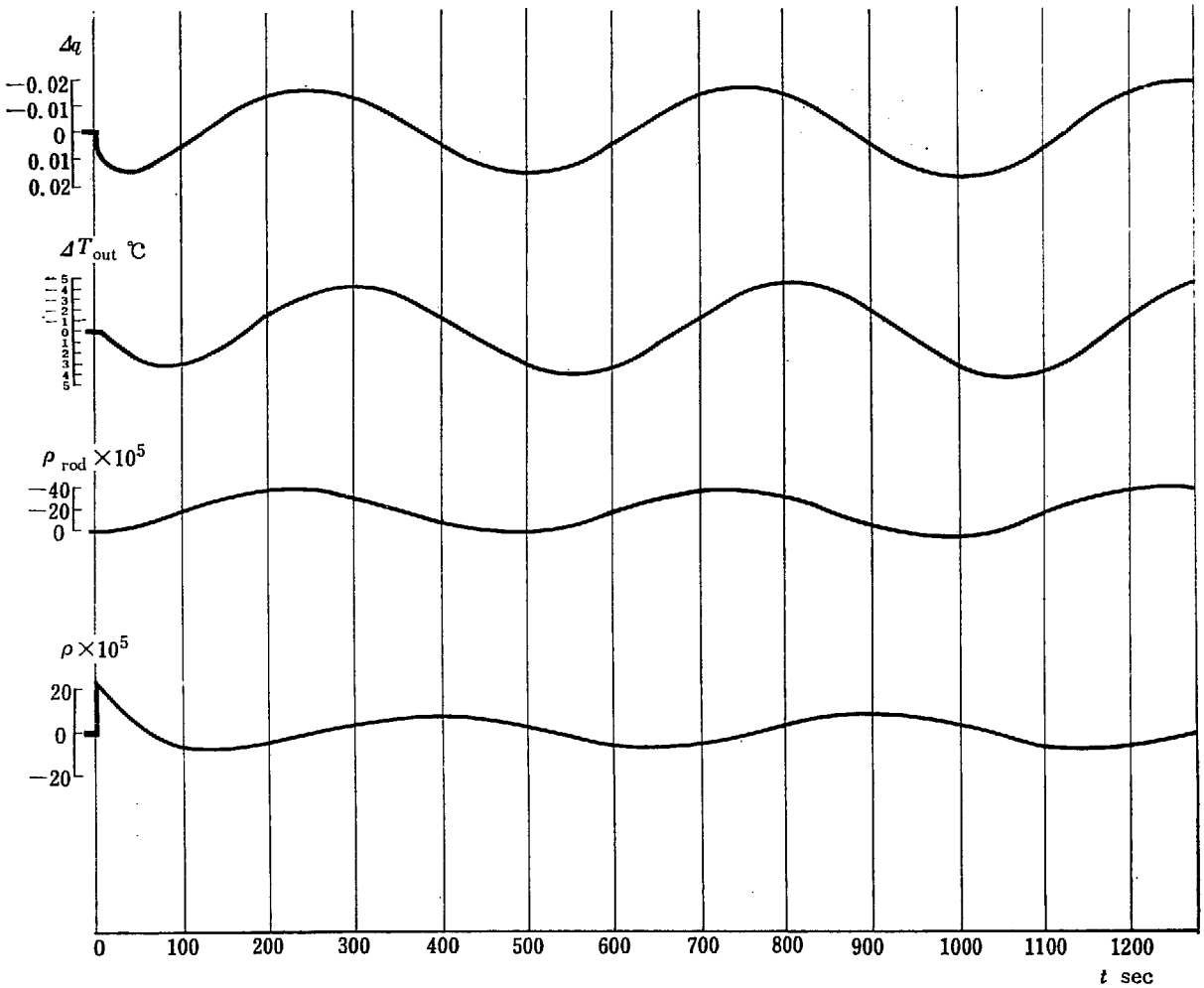

Fig. 4.1 (c) Examples of Transient Pesponses
$K=0.025\times10^{-5}$/sec °C
$T_I=80$ sec $T_D=30$ sec $\rho_{ex}=2\times10^{-4}$

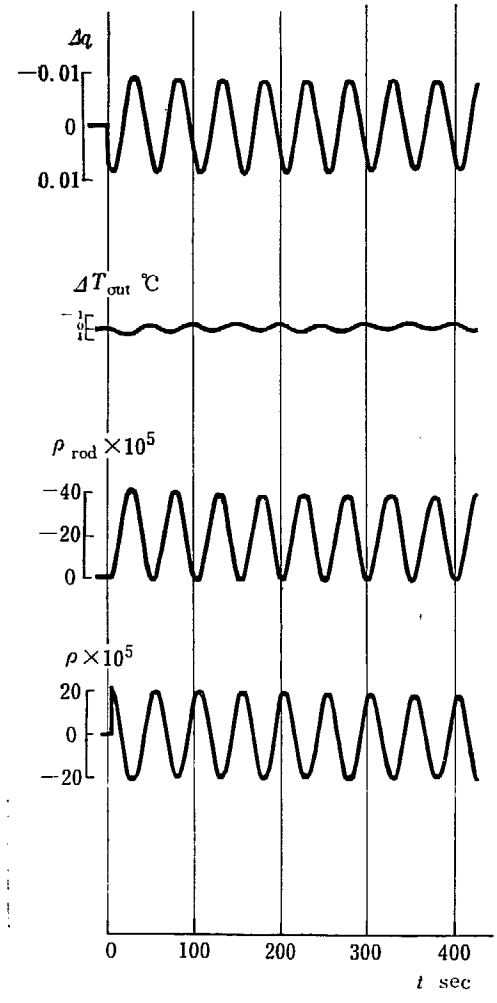

Fig. 4.2 (a) Examples of Transient Responses
$K=10^{-5}$/sec °C
$T_I=\infty$ $T_D=30$ sec $\rho_{ex}=2\times10^{-4}$

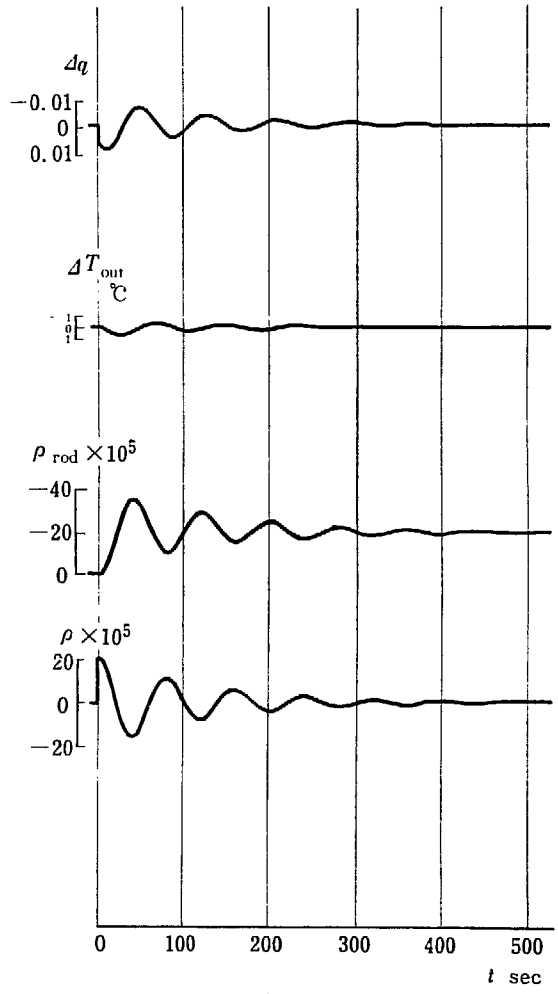

Fig. 4.2 (b) Examples of Transient Responses
$K=0.4\times10^{-5}$/sec °C
$T_I=\infty$ $T_D=30$ sec $\rho_{ex}=2\times10^{-4}$

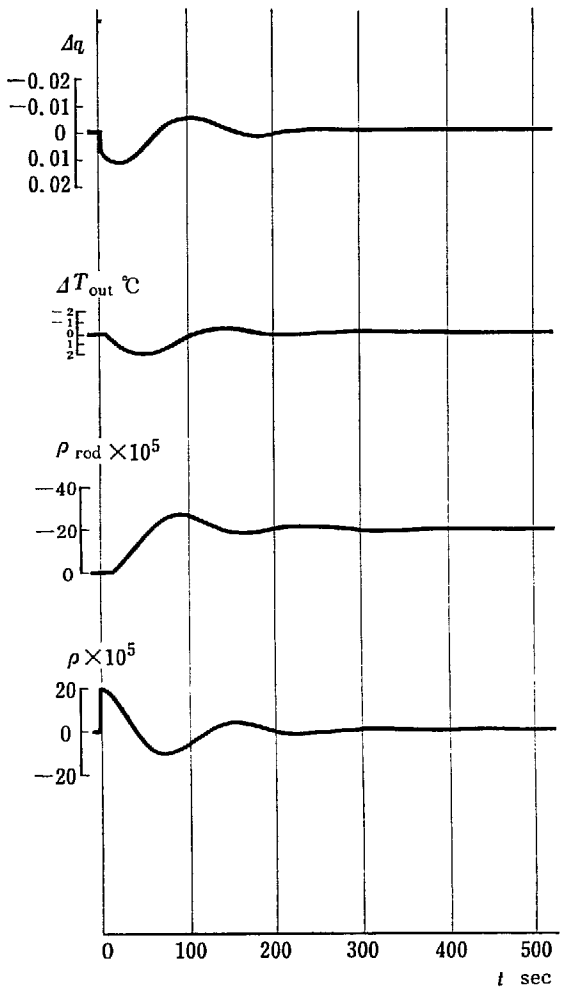

Fig. 4.2 (c) Examples of Transient Responses
$K=0.1\times10^{-5}$/sec °C
$T_I=\infty$ $T_D=30$ sec $\rho_{ex}=2\times10^{-4}$

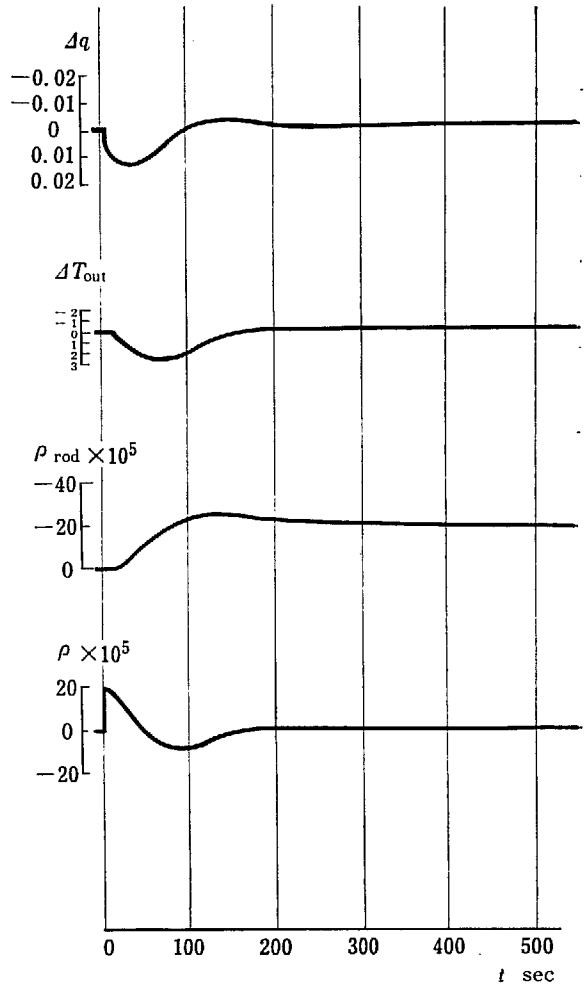

Fig. 4.2 (d) Examples of Transient Responses
$K=0.05\times10^{-5}$/sec °C
$T_I=\infty$ $T_D=30$ sec $\rho_{ex}=2\times10^{-4}$

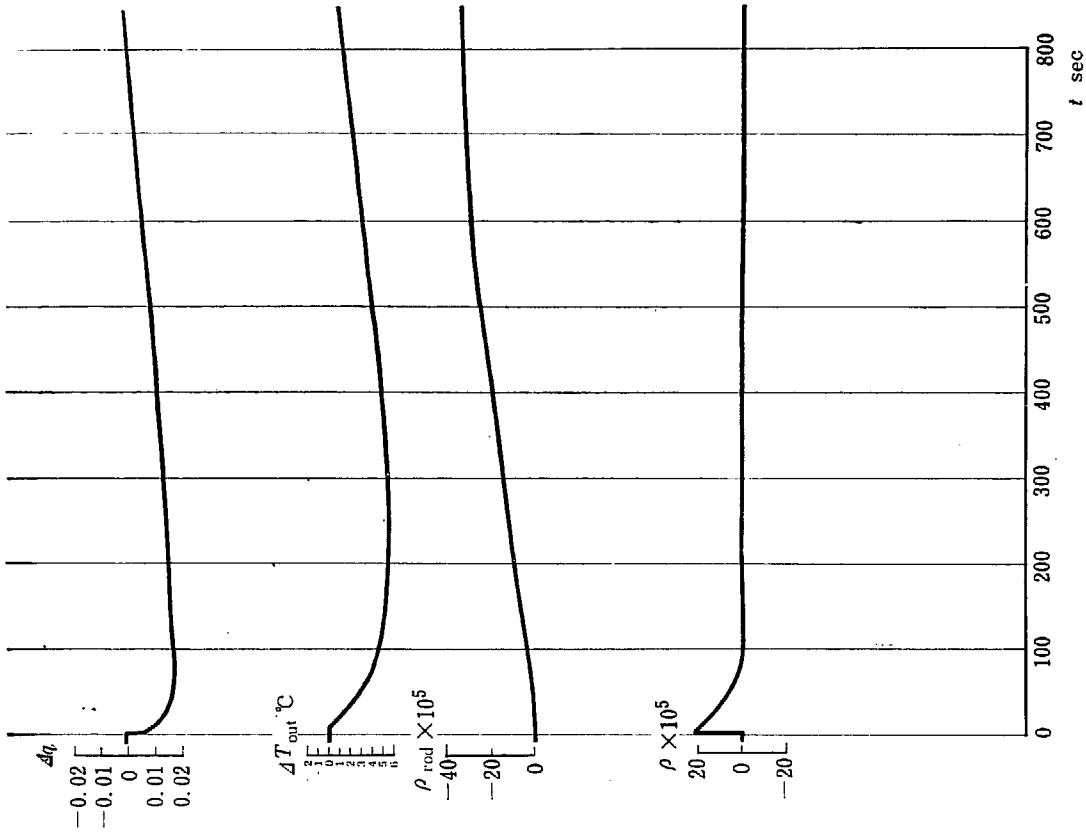

Fig. 4.2 (f) Examples of Transient Responses
$K = 0.005 \times 10^{-5}$/sec °C
$T_I = \infty$ $T_D = 30$ sec $\rho_{ex} = 2 \times 10^{-4}$

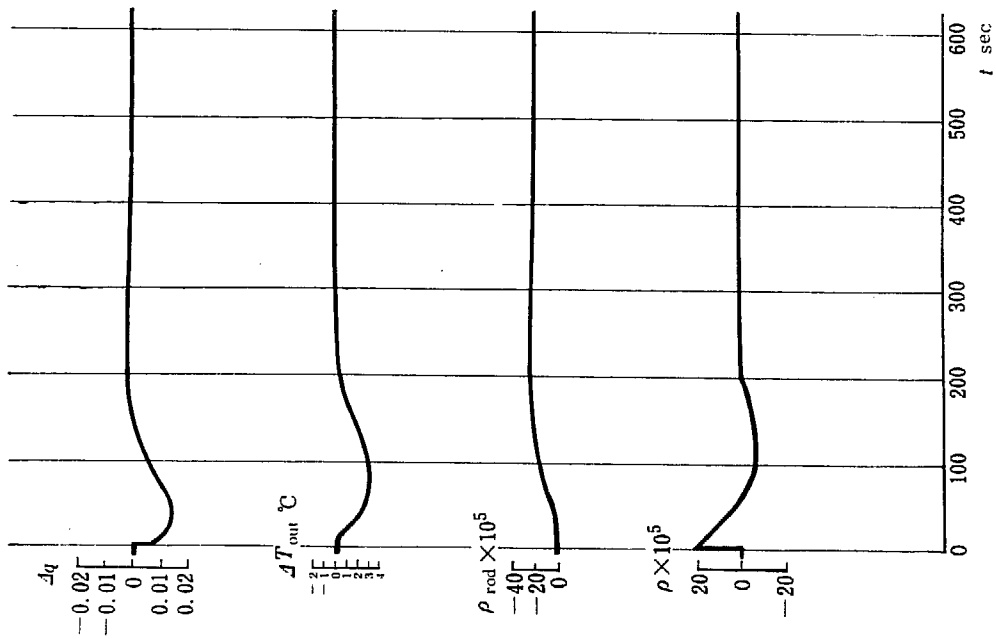

Fig. 2.4 (e) Examples of Transient Responses
$K = 0.03 \times 10^{-5}$/sec °C
$T_I = \infty$ $T_D = 30$ sec $\rho_{ex} = 2 \times 10^{-4}$

4.1.2 Optimum Phase Margins

As shown in **Fig. 4.2**, the indicial responses are quite sensitive to the controller gains. Therefore it is necessary, in designing the control system, to choose an optimum controller gain. A more detailed comparison of the indicial responses for different value of the controller gain is given in **Fig. 4.3**. The gain and the phase margins for each case are also shown. It is observed that $K=5\times10^{-7}$/sec °C is quite

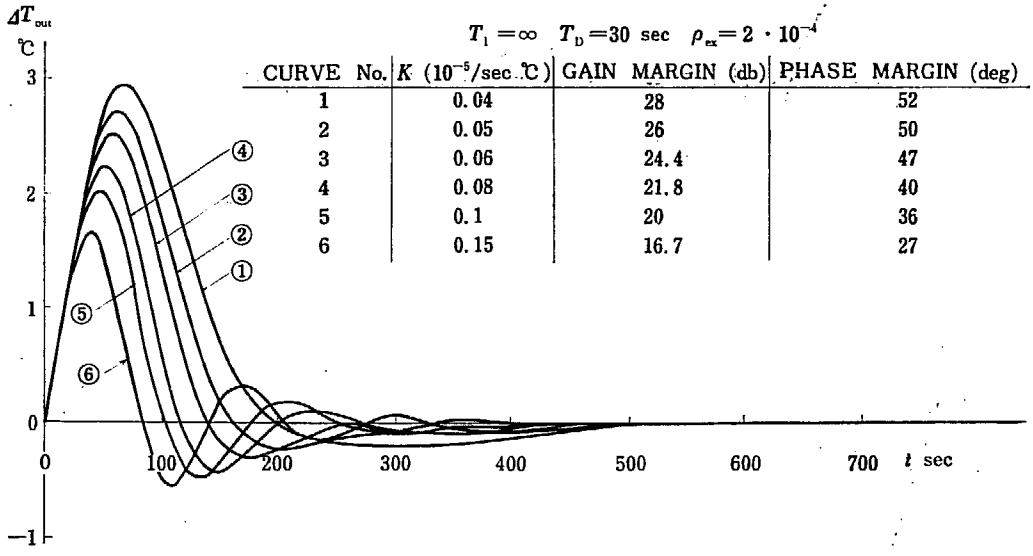

$T_I=\infty$ $T_D=30$ sec $\rho_{ex}=2\cdot10^{-4}$

CURVE No.	K (10^{-5}/sec ℃)	GAIN MARGIN (db)	PHASE MARGIN (deg)
1	0.04	28	52
2	0.05	26	50
3	0.06	24.4	47
4	0.08	21.8	40
5	0.1	20	36
6	0.15	16.7	27

Fig. 4.3 Effect of Varying K on Response of ΔT_{out}
$T_I=\infty$ $T_D=30$ sec $\rho_{ex}=2\times10^{-4}$ $K=0.04\sim0.15^{-5}$/sec °C

close to the optimum. It is said that the system response is optimum for a gain margin in the range of 10~20 db and for a phase margin in the range of 40~60 degrees.[6] The optimum values in this case are 26 db gain margin and 50 degree phase margin.

4.1.3 Effect of Varying Controller Constants

A series of figures show the effects of varying the controller constants, T_I and T_D, with the controller gain fixed at $K=5\times10^{-7}$/sec °C. From **Fig. 4.4**, it is noted that increase in T_D improves the responses. But the effect is not very pronounced if T_D is increased beyond 30 sec. One disadvantage of increasing T_D is that the system becomes more sensitive to noise. Therefore it is advisable to use $T_D=30$ sec, the lowest value of T_D for which the system response is satisfactory.

The effect of varying T_I is shown in **Fig. 4.5**. The best response is obtained for $T_I=\infty$. Even for $T_I=160$ sec, damping of the transients is quite poor. For the value of T_I as low as 40 sec, the response diverges.

Thus it is verified that $T_I=\infty$ and $T_D=30$ sec, as assumed in obtaining **Fig. 4.3**, is an optimum combination of the controller constants.

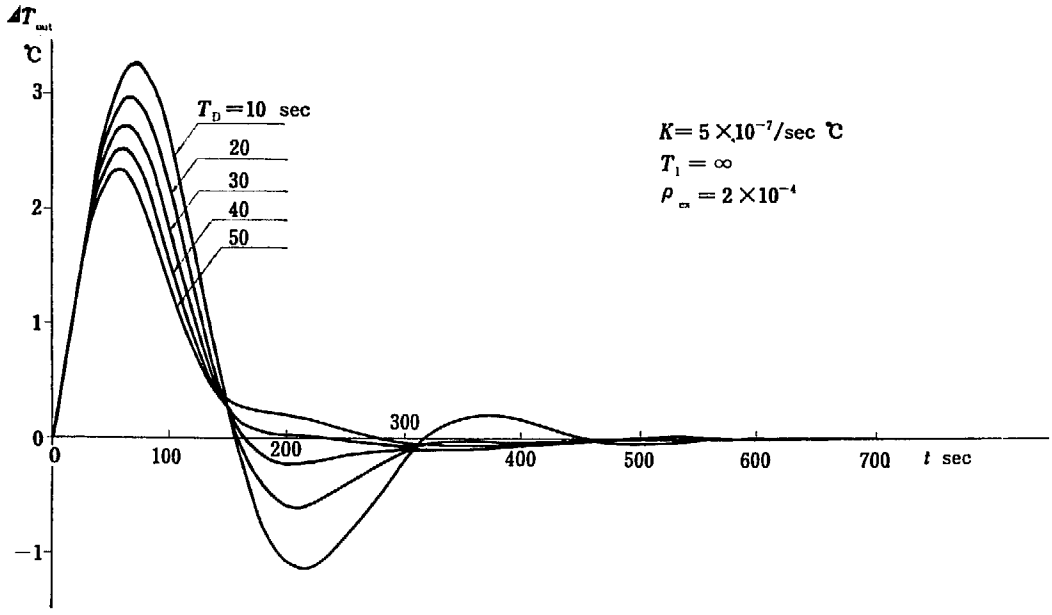

(a) Effect of Varying T_D on Response of T_{out}

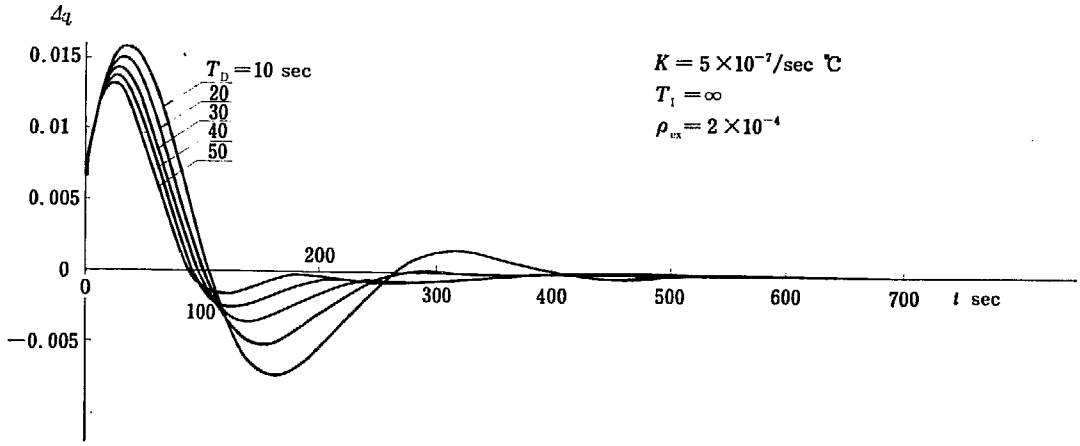

(b) Effect of Varying T_D on Response of Δq

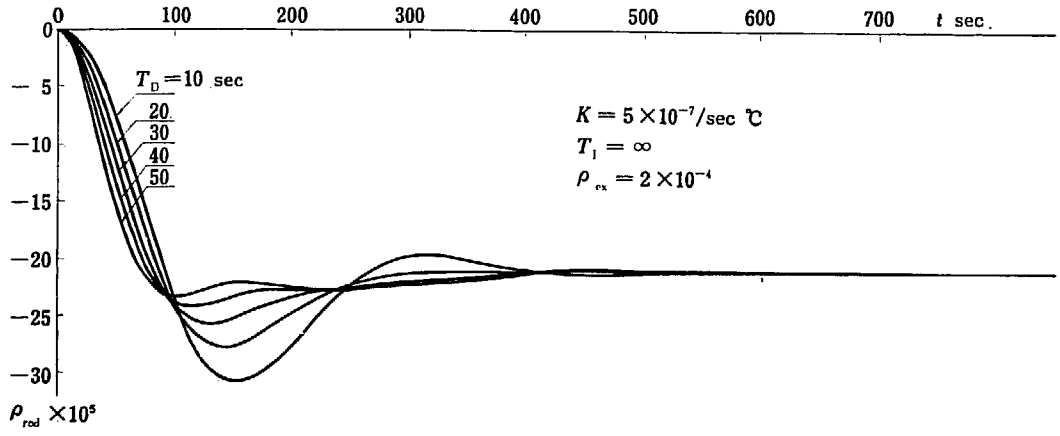

(c) Effect of Varying T_D on Response of ρ_{rod}

Fig. 4.4 Effect of Varying T_D on Responses
$K=5\times10^{-7}$/sec °C $T_I=\infty$ $\rho_{ex}=2\times10^{-4}$ $T_D=10\sim50$ sec

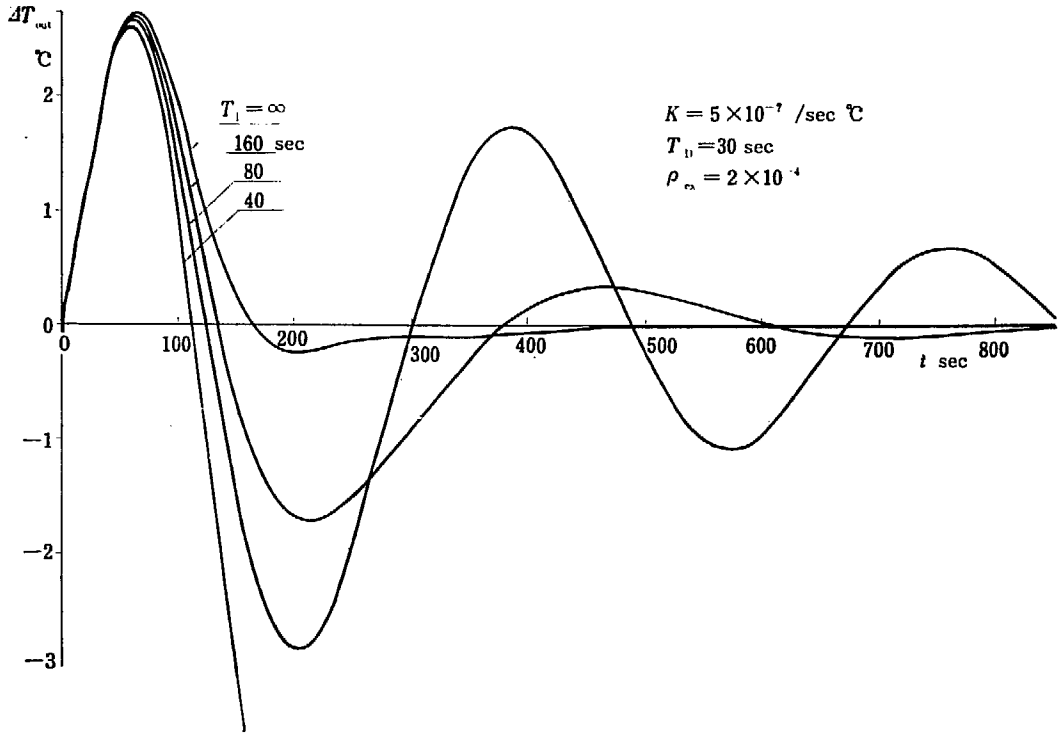

Fig. 4.5 (a) Effect of Varying T_I on Response of ΔT_{out}
$K=5\times10^{-7}$/sec °C $T_D=30$ sec $\rho_{ex}=2\times10^{-4}$ $T_I=40$ sec$\sim\infty$

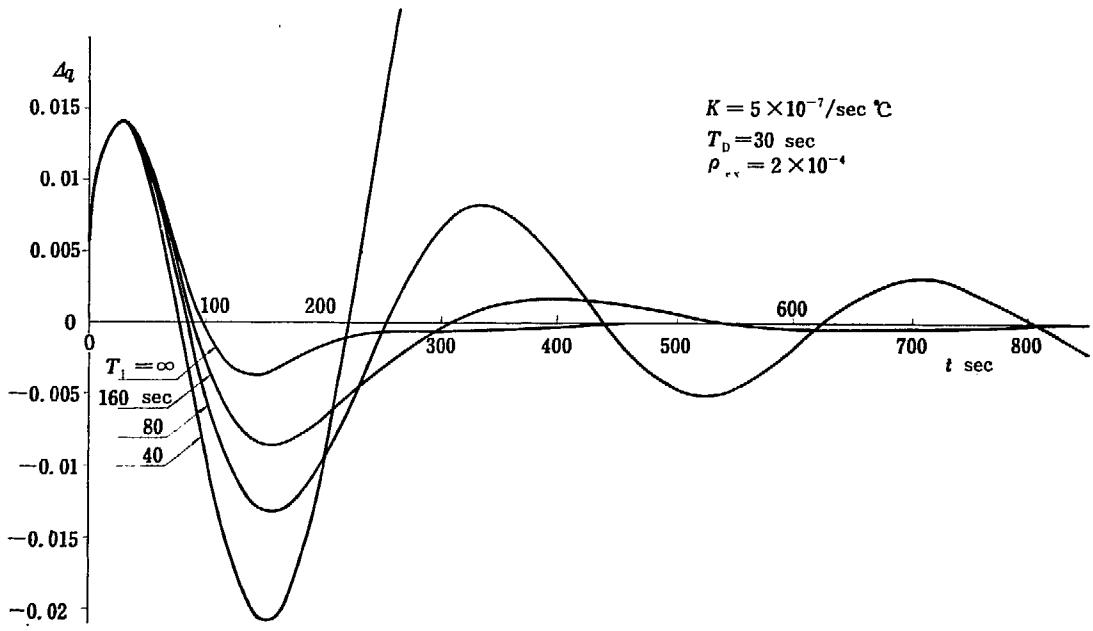

Fig. 4.5 (b) Effect of Varying T_I on Response of Δq
$K=5\times10^{-7}$/sec °C $T_D=30$ sec $\rho_{ex}=2\times10^{-4}$ $T_I=40$ sec$\sim\infty$

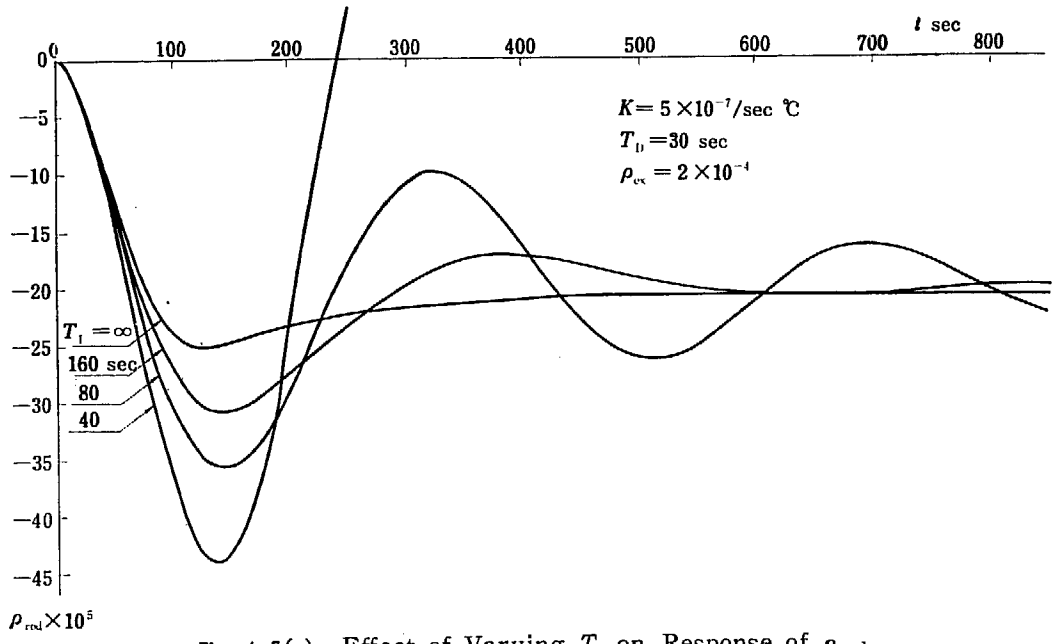

Fig. 4.5(c) Effect of Varying T_I on Response of ρ_{rod}
$K=5\times10^{-7}$/sec °C $T_D=30$ sec $\rho_{ex}=2\times10^{-4}$ $T_I=40$ sec$\sim\infty$

4.1.4 Effect of Rod Speed Limit

It is sometimes necessary from the reactor safety viewpoint to limit the control rod speed. The effect of the rod speed limits is shown in Fig. 4.6 for the optimum settings of the controller. The disturbance is assumed to be 2×10^{-4} in reactivity. It is noticed that if the speed limit is larger than 0.34×10^{-5}/sec, the rod speed does not reach its maximum and, therefore, the response is the same as that obtained before. If the speed limit is set at $R_{max}=0.2\times10^{-5}$/sec, the rod speed does reach its maximum, but the response is not so much different. For the speed limit

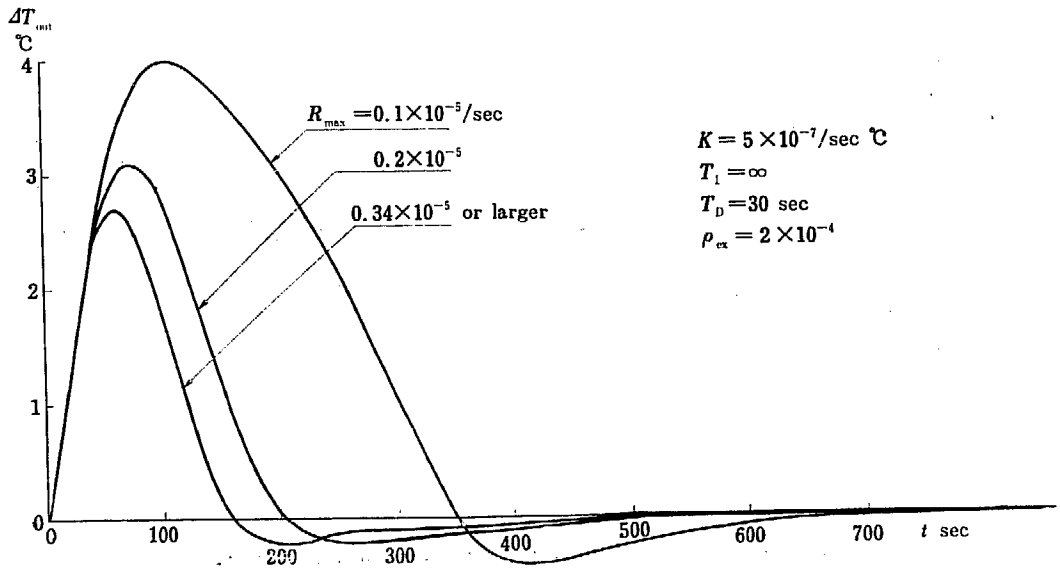

Fig. 4.6 Effect of Rod Speed Limit on Response of ΔT_{out}

as low as $R_{max}=0.1\times10^{-5}$/sec, the system response is quite poor.

The reasonable value of the speed limit to be used in actual reactors will probably be of the order of 10^{-5}/sec and hence it will little affect the system response unless an excessive amount of disturbance is introduced.

Fig. 4.7 shows an example of responses with rod speed limits.

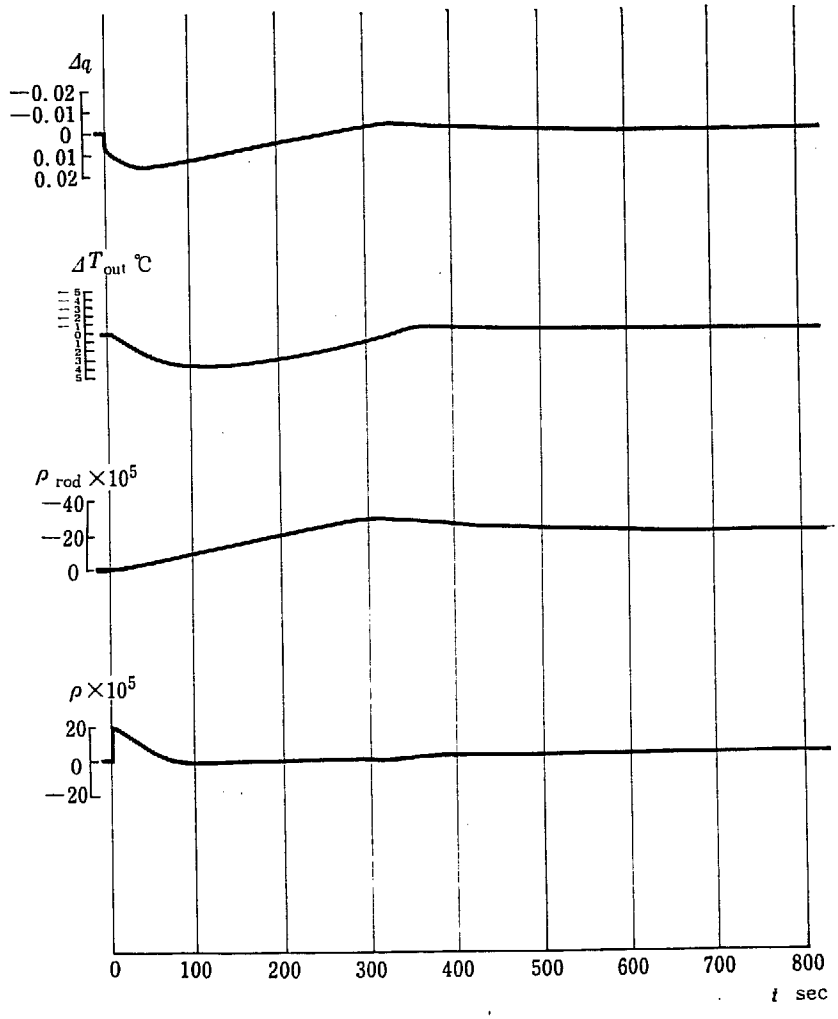

Fig. 4.7 Example of Transient Responses

$K=5\times10^{-7}$/sec °C $T_I=\infty$ $T_D=30$ sec $\rho_{ex}=2\times10^{-4}$ $R_{max}=0.1\times10^{-5}$/sec

4.2 Discontinuous Control

As anticipated from the vector locus analysis, the system undergoes sustained oscillations corresponding to the stables limit cycles. **Fig. 4.8** and **4.9** show examples of transient responses. The transient response shown in **Fig. 4.8** is the low frequency oscillation corresponding to the limit cycle L_1. The high frequency oscillation of L_3 is shown in **Fig. 4.9**. The frequency and amplitude of the oscillation as functions of the controller gain are shown in **Fig. 4.10**. It is observed from this figure that the frequency and the amplitude of the lower limit cycle L_1 are almost independent of the controller gain, while the amplitude of the higher limit

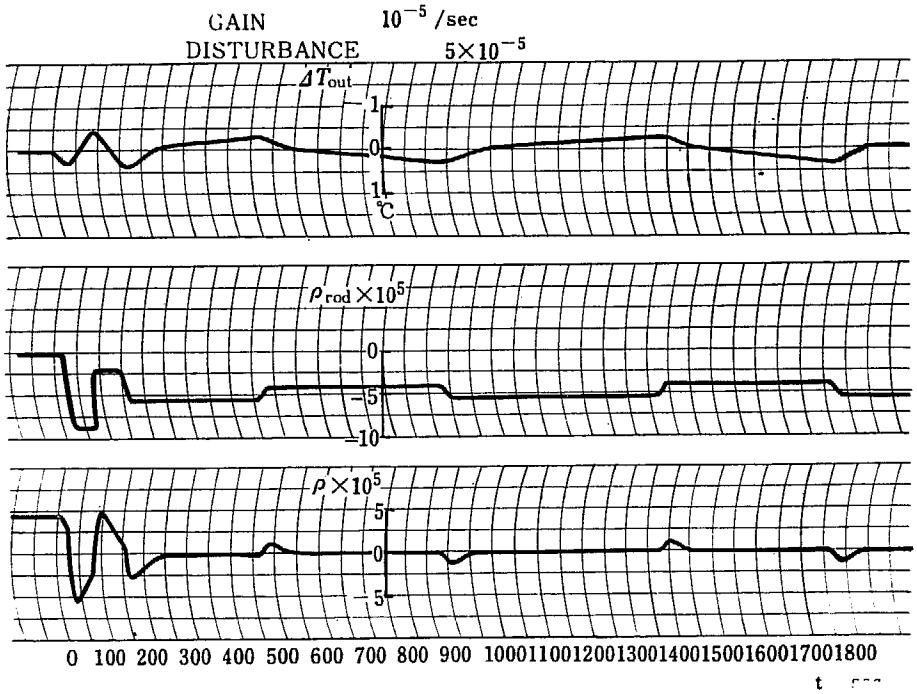

Fig. 4.8 Example of Transient Responses
$K_d=10^{-5}$/sec $T_I=80$ sec $T_D=30$ sec $\rho_{ex}=5\times10^{-5}$

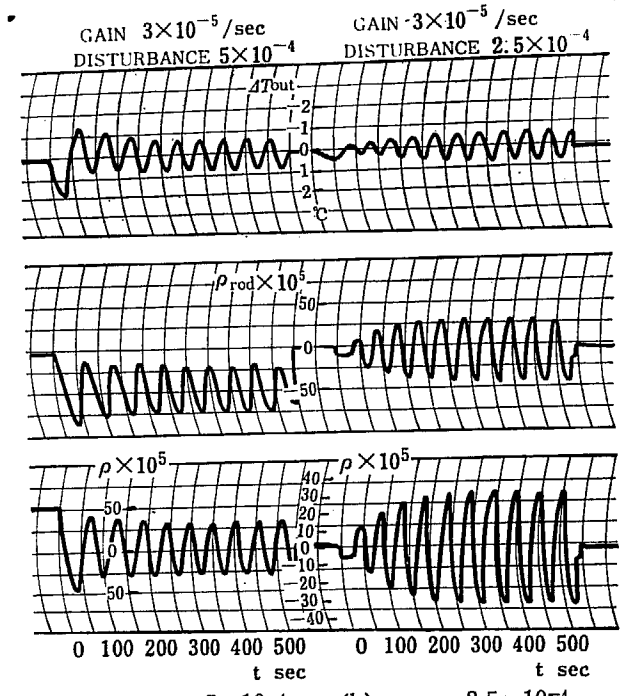

(a) $\rho_{ex}=5\times10^{-4}$ (b) $\rho_{ex}=2.5\times10^{-4}$

Fig. 4.9 Examples of Transient Responses
$K_d=3\times10^{-5}$/sec $T_I=80$ sec $T_D=30$ sec

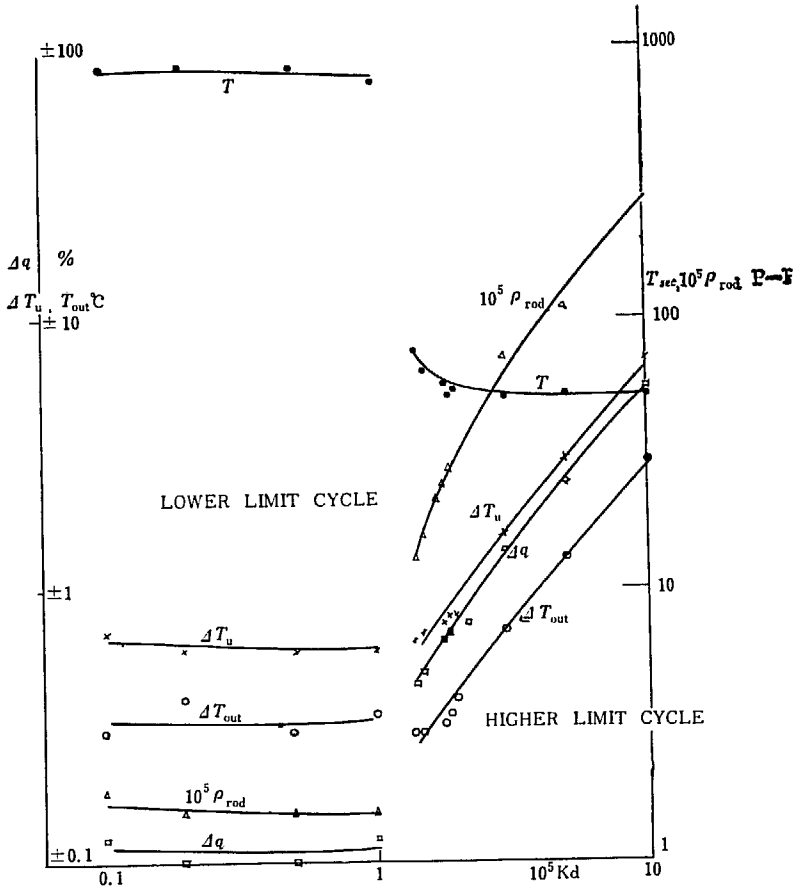

Fig. 4.10 Relationship of Amplitude and Frequency of Limit Cycles to Controller Gain

cycle L_3 increases with increasing controller gain. The frequency of L_3 is also almost independent of the gain and about ten times as high as that of L_1. From the analysis by the describing function method it is concluded that the frequency of oscillation is 0.125 rad/sec for L_3 and 0.0122 rad/sec for L_1 and is independent of the gain and that the amplitude of L_1 decreases and that of L_3 increases with the increasing gain. Therefore, there are some discrepancies between the results of analog computer studies and the conclusions of the describing function method. They may be ascribed to the fact that only the fundamental component of oscillations is considered in the describing function method. The traces in Figs. 4.8 and 4.9 are quite different from sinusoidal waves and it is understandable that taking only the fundamental component is rather crude an approximation. It might be concluded that the describing function method is good enough to anticipate the qualitative behavior of the system, such as the stability and the existence of limit cycles, but is too crude to discuss the frequency or amplitude of oscillation quantitatively.

In Fig. 4.11 is shown the relationship between the maximum value of the reactivity disturbance, below which the system does not diverge, and the controller gain. It is noted that for the controller gain of $K_d=10^{-6}$/sec the system diverges

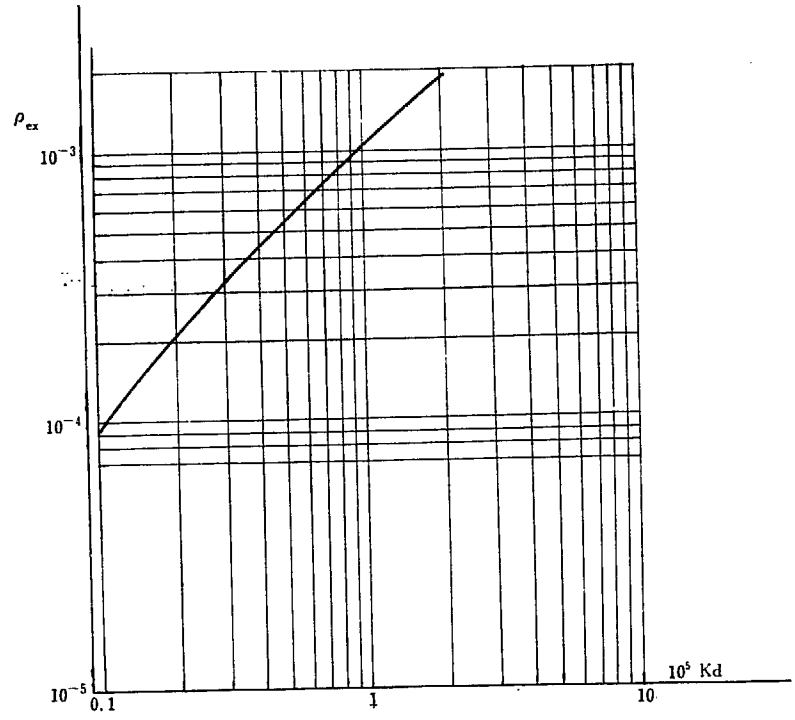

Fig. 4.11 Relationship of Maximum Allowable Disturbance to Controller Gain

if the disturbance is larger than 10^{-4}. The maximum allowable disturbance, however, increases almost proportionally to the controller gain and, therefore, the system does not diverge for $K_d=10^{-5}$/sec unless the disturbance exceeds 10^{-3}. Since it is not likely that the magnitude of the disturbance exceeds 10^{-3} during normal operation, the discontinuous control system will work satisfactorily if the controller gain is 10^{-5}/sec or higher.

4.3 Continuous Control with Position Feedback

4.3.1 Stability Limit

If $KK_{f2}>17$ db, the system becomes unstable. This is illustrated in Fig. 4.12. (a), where $K=7\times10^{-5}$/sec °C and $K_{f2}=10^{+5}$/sec °C. A high frequency divergent oscillation is observed.

A low frequency oscillation due to too low a gain is illustrated in Fig. 4.12 (b).

4.3.2 Effect of Varying Controller Constants

The effect of varying the controller constants, T_I and T_D is illustrated in Figs. 4.13 and 4.14. It is noted that for large T_D the response is quite oscillatory and $T_D=20$ sec seems to give the best response. From Fig. 4.14 it is observed that if $T_I=\infty$ there is some residual error in the responses of ΔT_{out} and Δq. In the basic system of Sec. 3.1 the controller contains an integral action due to $1/s$ term in the motor transfer function and, therefore, there is no residual error in ΔT_{out} even if $T_I=\infty$. If the rod position feedback is used, the $1/s$ term in the controller transfer function is eliminated as is shown in Eq. (3.6). Hence, if $T_I=\infty$, the con-

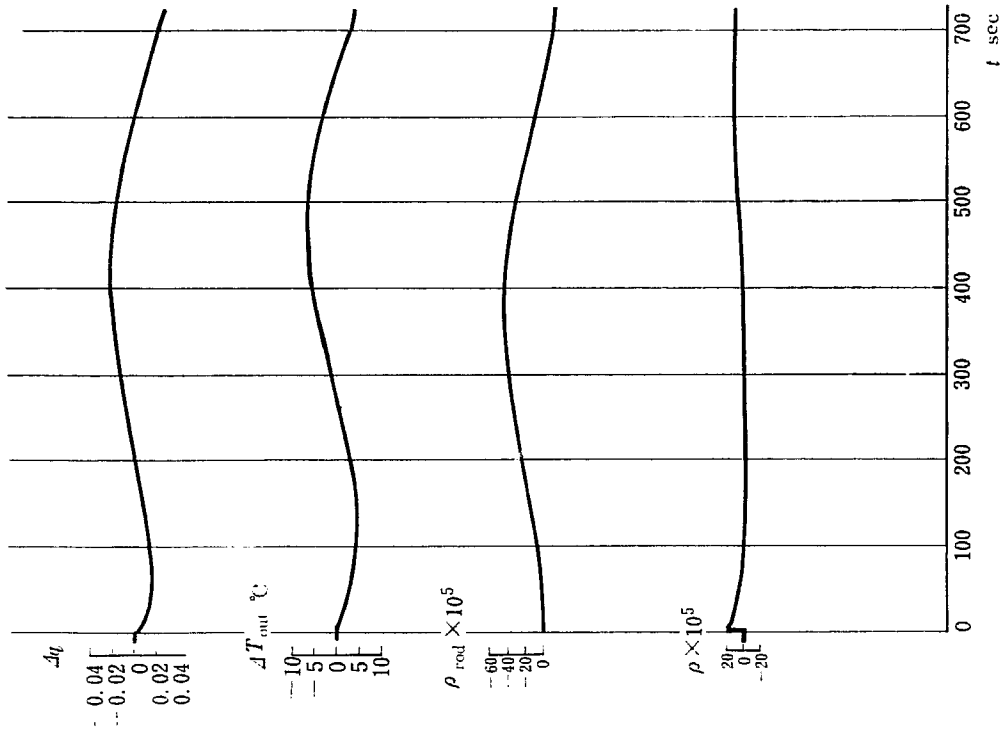

Fig. 4.12 (b) Example of Transient Responses
$K=10^{-7}$/sec °C $K_{f2}=10^{+4}$ °C $T_I=80$ sec
$T_D=20$ sec. $\rho_{ex}=2\times10^{-4}$

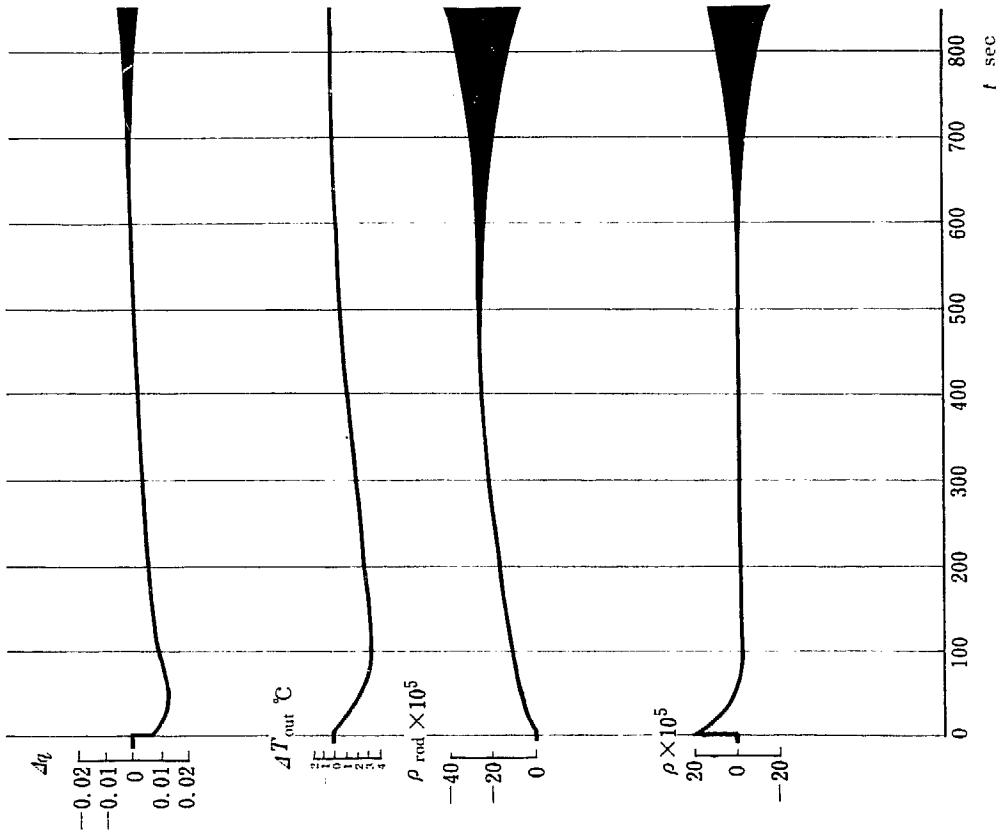

Fig. 4.12 (a) Example of Transient Responses
$K=7\times10^{-5}$/sec °C $K_{f2}=10^{+5}$ °C $T_I=80$ sec
$T_D=30$ sec. $\rho_{ex}=2\times10^{-4}$

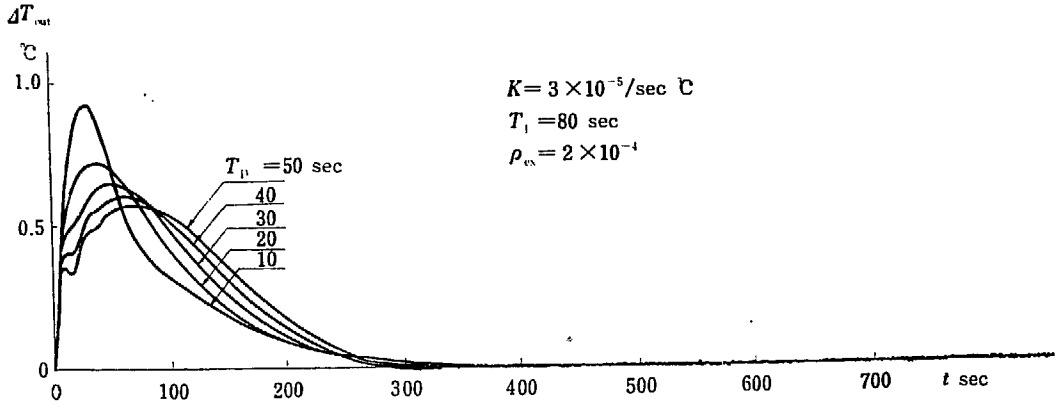

(a) Effect of Varying T_D on Response of ΔT_{out}

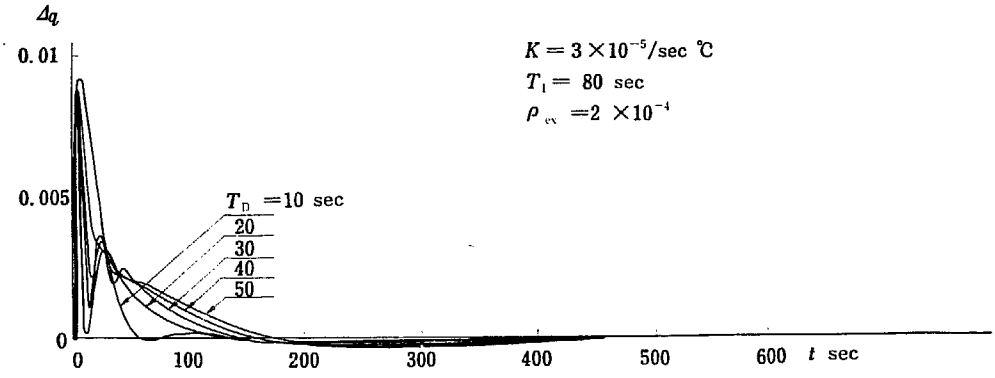

(b) Effect of Varying T_D on Response of Δq

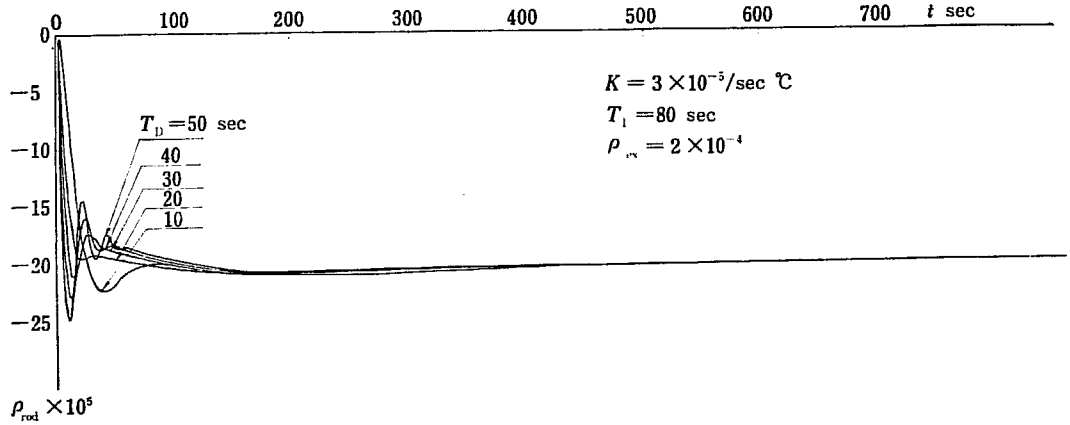

(c) Effect of Varying T_D on Response of ρ_{rod}

Fig. 4.13 Effect of Varying T_D on Response

$K=3\times10^{-5}$/sec °C $K_{f2}=10^{+4}$ °C $T_I=80$ sec $T_D=10\sim50$ sec $\rho_{ex}=2\times10^{-4}$

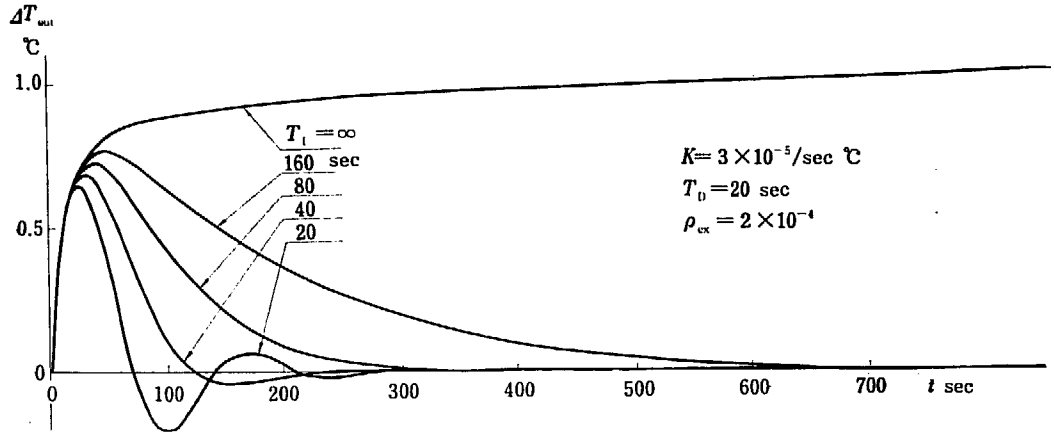

(a) Effect of Varying T_I on Response of ΔT_{out}

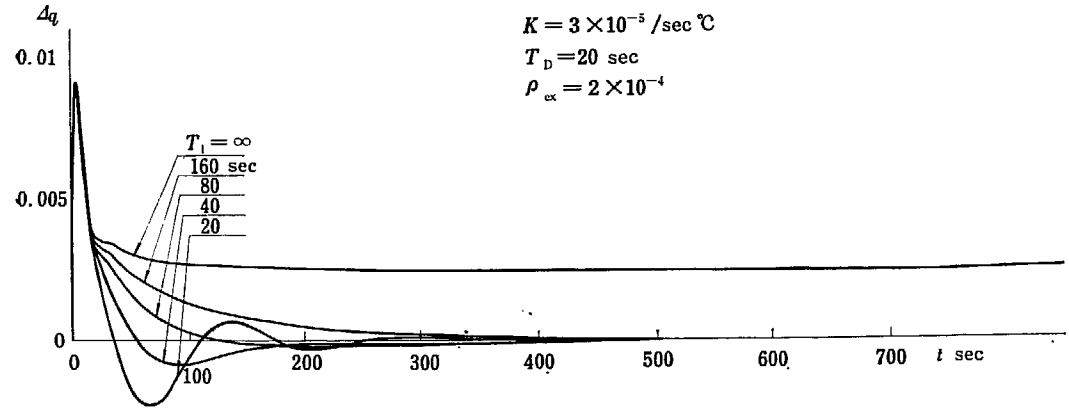

(b) Effect of Varying T_I on Response of Δq

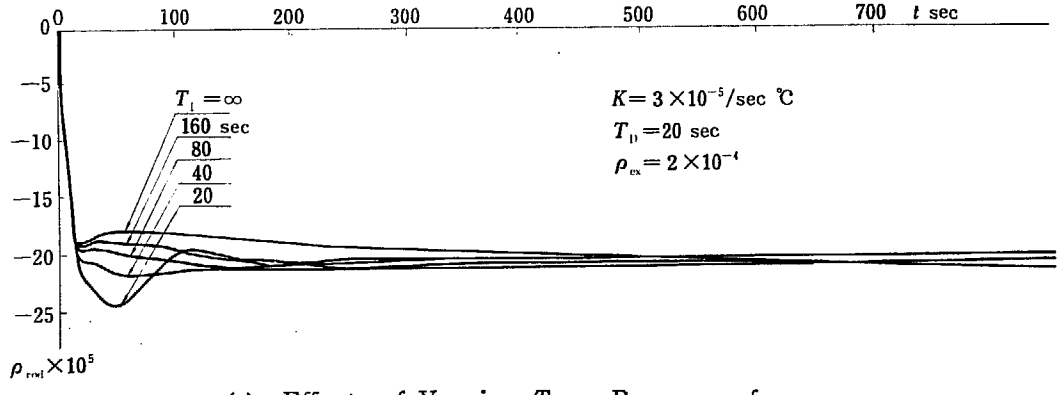

(c) Effects of Varying T_I on Response of ρ_{rod}

Fig. 4.14 Effects of Varying T_I on Response

$K = 3 \times 10^{-5}$/sec °C $K_{f2} = 10^{+4}$ °C $T_D = 20$ sec $\rho_{ex} = 2 \times 10^{-4}$ $T_I = 20$ sec$\sim\infty$

troller does not include integral action at all and the residual error results. Figure 4.14 shows that T_I=80 sec is nearly optimum, the response is fast enough without an excessive overshoot. The response for T_I=40 sec is also quite good.

Thus the optimum controller settings are

T_I=40~80 sec

T_D=20 sec

for this case, while for the basic system they were

T_I=∞

T_D=30 sec

4.3.3 Effect of Varying K_{f2} and K

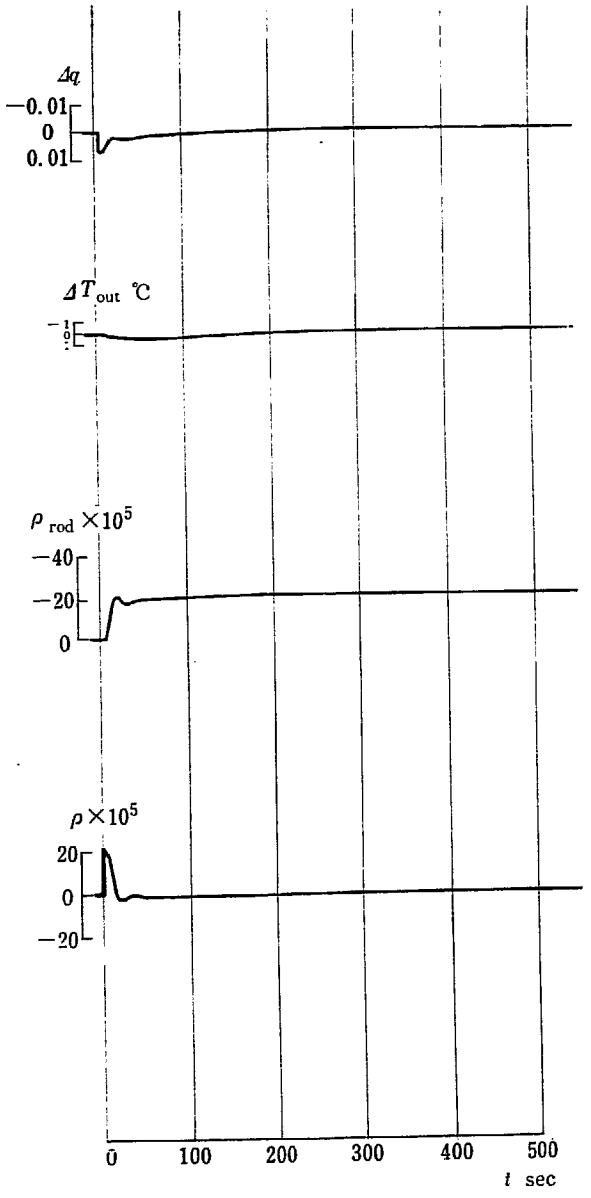

(a) $K_{f2}=10^{+4}$ °C

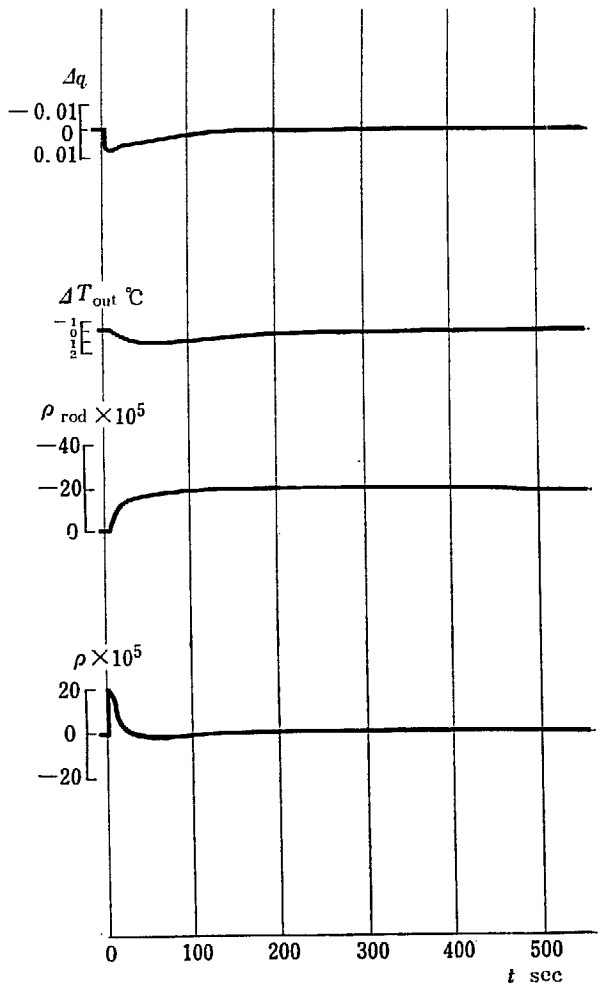

(b) $K_{f2}=2\times10^{+4}$ °C

Fig. 4.15 Examples of Transient Responses
$K=3\times10^{-5}$/sec °C T_I=80 sec T_D=30 sec $\rho_{ex}=2\times10^{-4}$

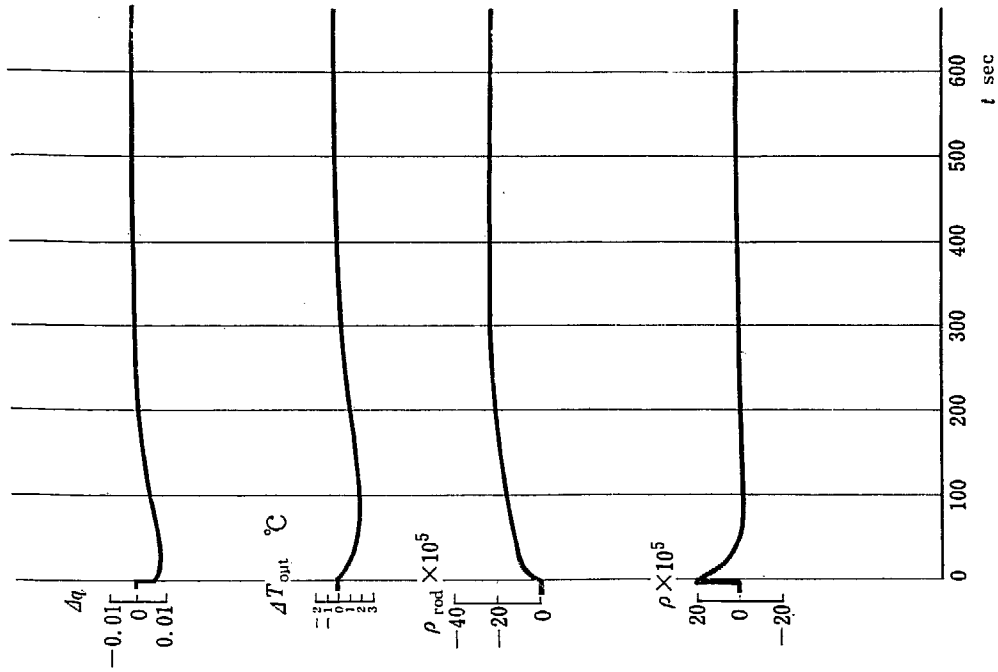

(d) $K_{f2}=10^{+5}$ °C

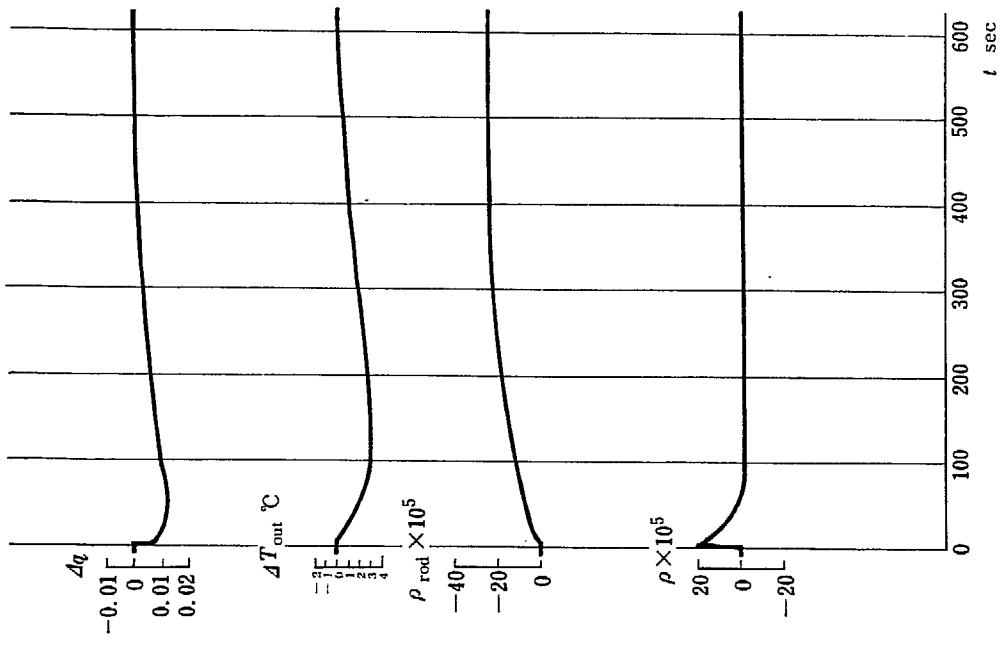

(c) $K_{f2}=5\times10^{+4}$ °C

Fig. 4.15 Examples of Transient Responses
$K=3\times10^{-5}$/sec °C $T_I=80$ sec $T_D=30$ sec $\rho_{ex}=2\times10^{-4}$

In the basic system, an optimum combination of three parameters, T_I, T_D and the gain K, had to be obtained. In the present system, an additional parameter, K_{f2}, must be taken into consideration. The effect of varying K_{f2} on the responses are shown in **Figs. 4.15** and **4.16**. From **Fig. 4.16** it is observed that for $K=3\times10^{-7}$/sec °C, the feedback gain as high as $K_{f2}=5\times10^4$ °C gives a good result. For higher controller gain, the optimum value of K_{f2} decreases; namely, $K_{f2}=2\times10^4$ °C for $K=3\times10^{-6}$/sec °C and $K_{f2}=10^4$ °C for $K=3\times10^{-5}$/sec °C. Of all the responses, the one for $K=3\times10^{-5}$/sec °C and $K_{f2}=10^4$ °C seems to be the best. A more detailed comparison is made in **Fig. 4.16 (d)**, for $K=3\times10^{-5}$/sec °C and several different values of K_{f2} in the vicinity of $K_{f2}=10^4$ °C. It is noted that $K_{f2}=10^4$ °C is optimum, the response has a sufficient damping without excessive overshoot.

The effect of varying K are shown in **Fig. 4.17** and **Fig. 4.18**. For $K_{f2}=10^4$ °C, the effect of varying K is quite distinct. The system even diverges for the gain

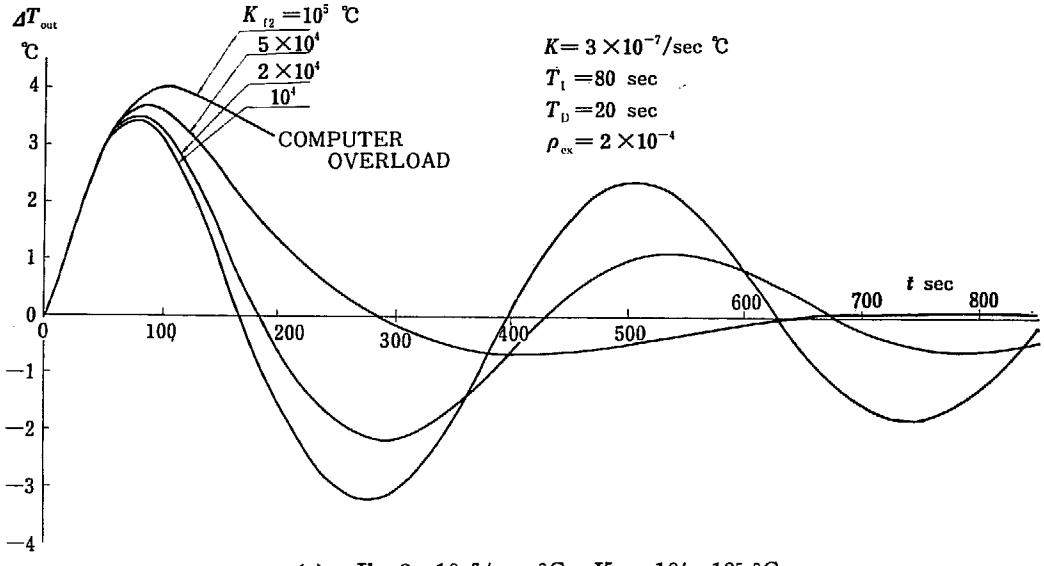

(a) $K=3\times10^{-7}$/sec °C $K_{f2}=10^4\sim10^5$ °C

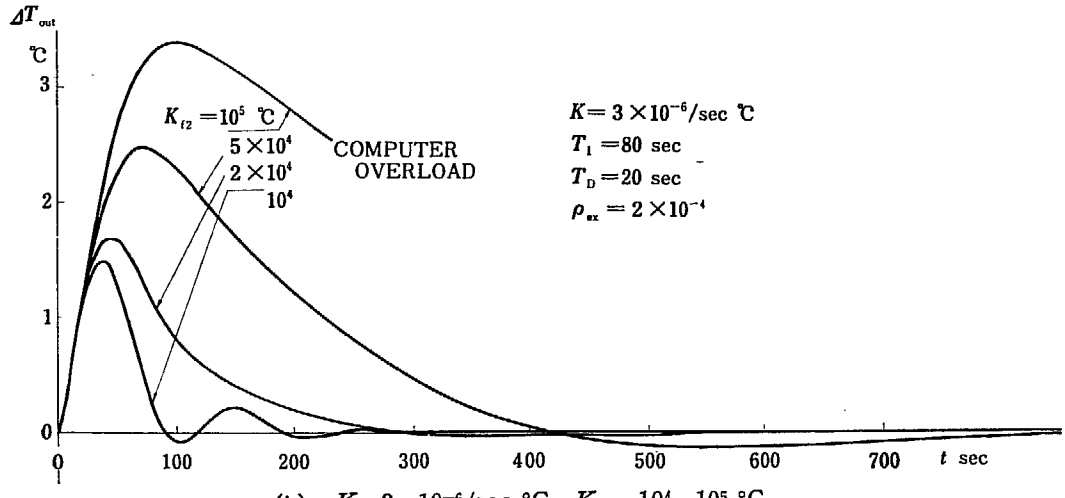

(b) $K=3\times10^{-6}$/sec °C $K_{f2}=10^4\sim10^5$ °C

Fig. 4.16 Effect of Varying K_{f2} on Response
$T_I=80$ sec $T_D=20$ sec $\rho_{ex}=2\times10^{-4}$

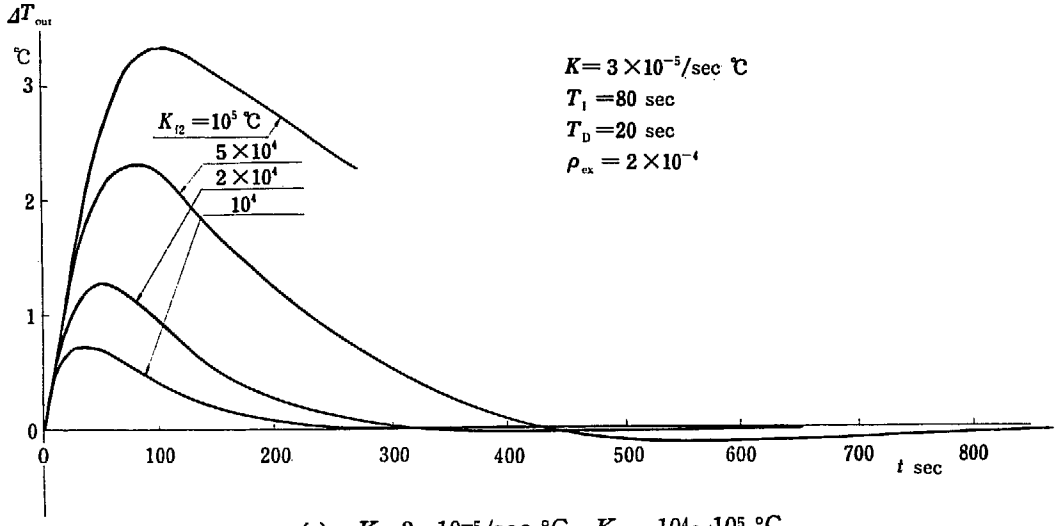

(c) $K=3\times10^{-5}$/sec °C $K_{f2}=10^4\sim10^5$ °C

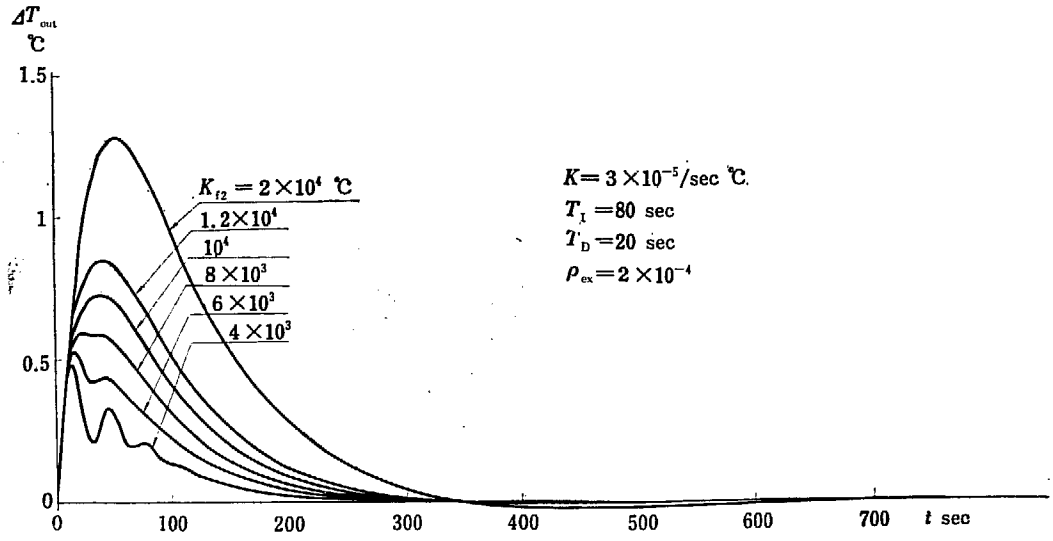

(d) $K=3\times10^{-5}$/sec °C $K_{f2}=4\times10^3\sim2\times10^4$ °C

Fig. 4.16 Effect of Varying K_{f2} on Response
$T_I=80$ sec $T_D=20$ sec $\rho_{ex}=2\times10^{-4}$

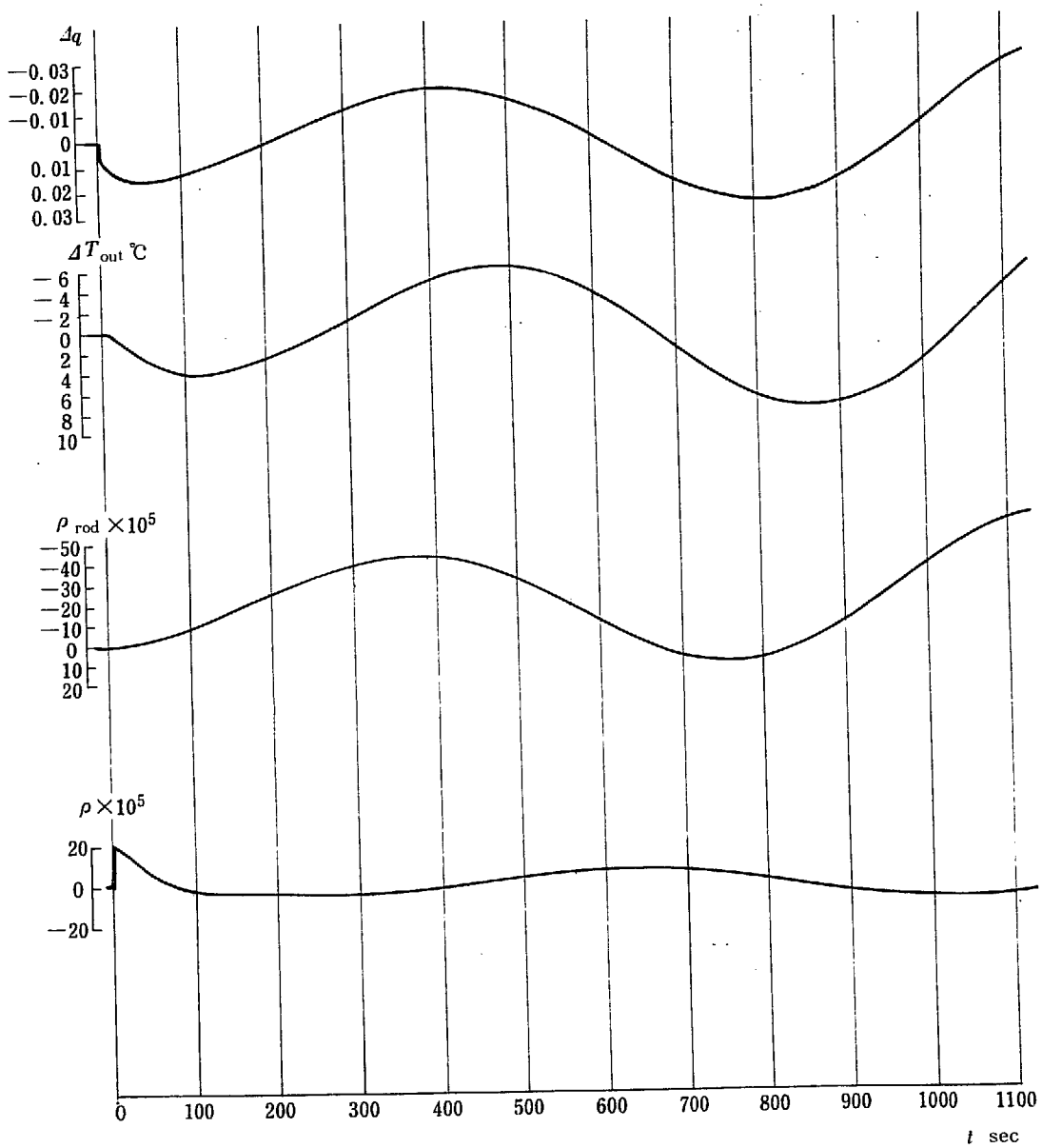

Fig. 4.17 (a) Examples of Transient Responses

$K=10^{-7}$/sec °C

$K_{f2}=10^4$ °C $T_I=80$ sec $T_D=30$ sec $\rho_{ex}=2\times10^{-4}$

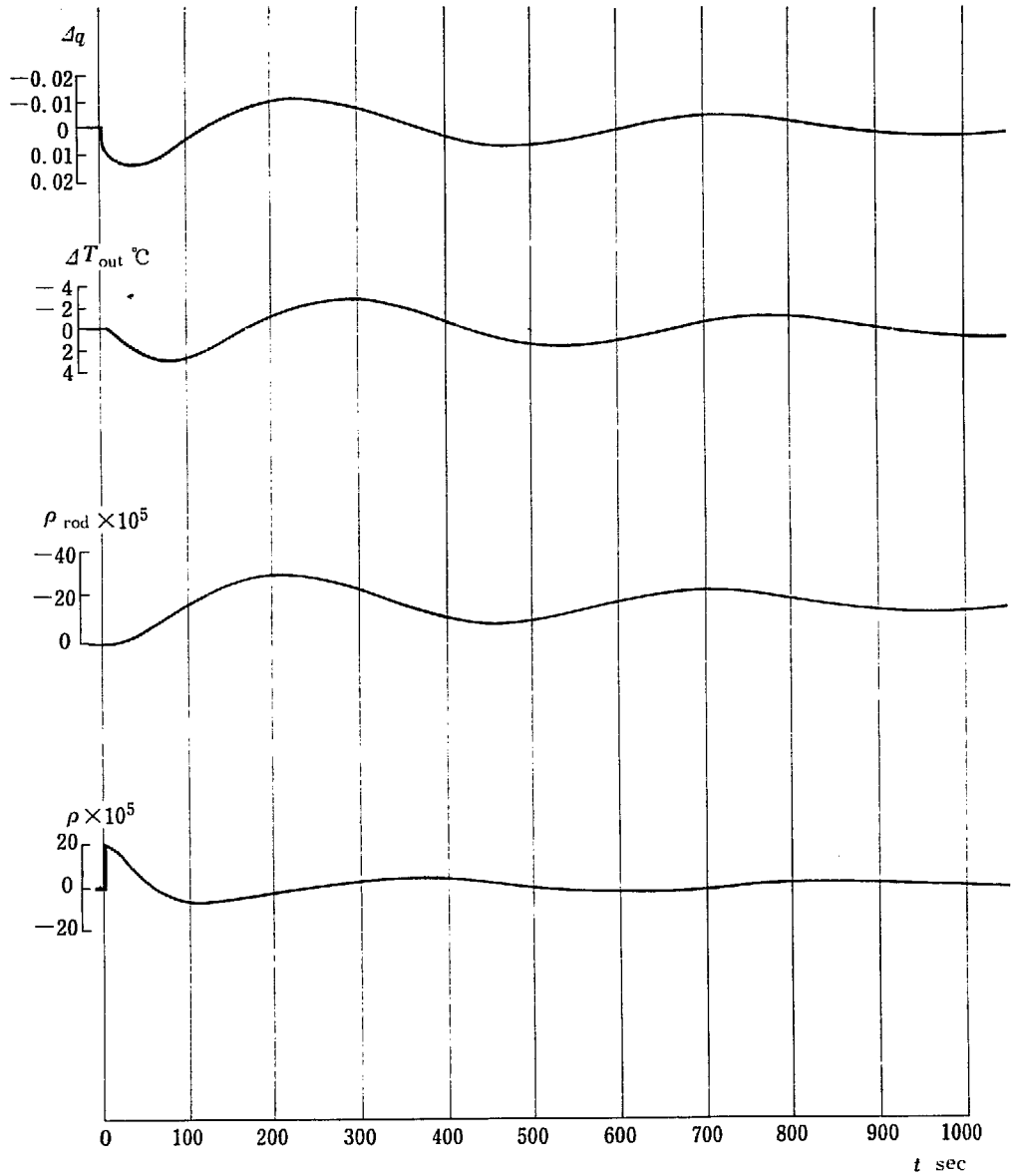

Fig. 4.17 (b) Examples of Transient Responses
$K=3\times10^{-7}$/sec °C
$K_{f2}=10^4$ °C $T_I=80$ sec $T_D=30$ sec $\rho_{ex}=2\times10^{-4}$

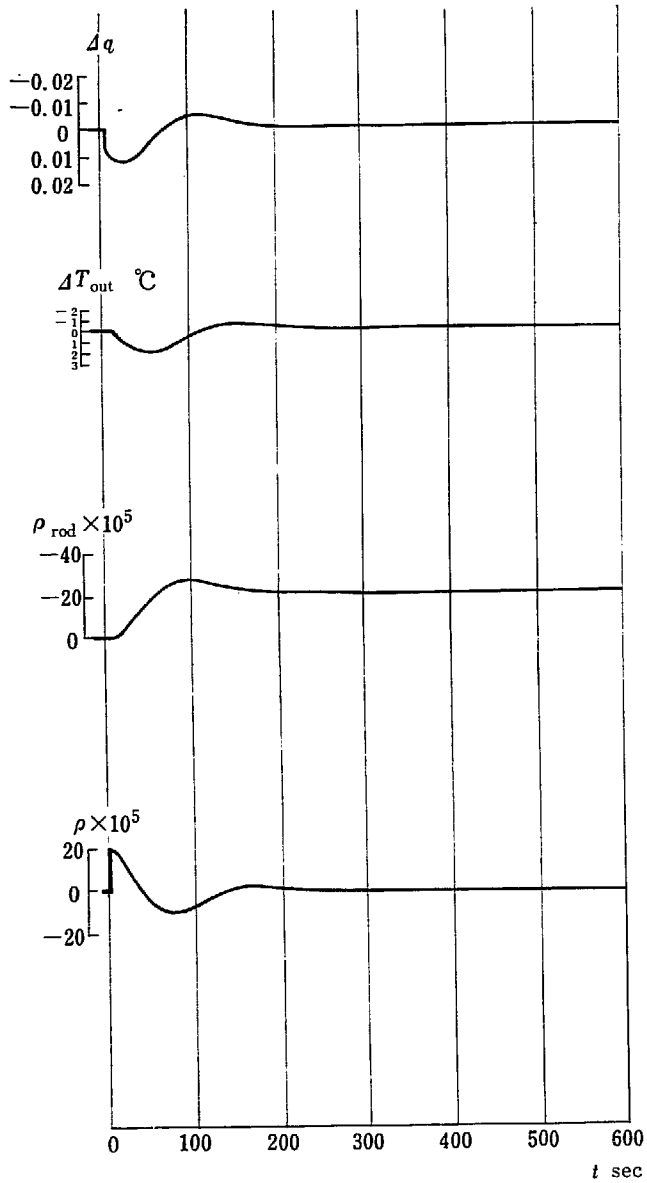

Fig. 4.17 (c) Examples of Transient Responses
$K=10^{-6}$/sec °C
$K_{f2}=10^4$ °C $T_I=80$ sec $T_D=30$ sec $\rho_{ex}=2\times10^{-4}$

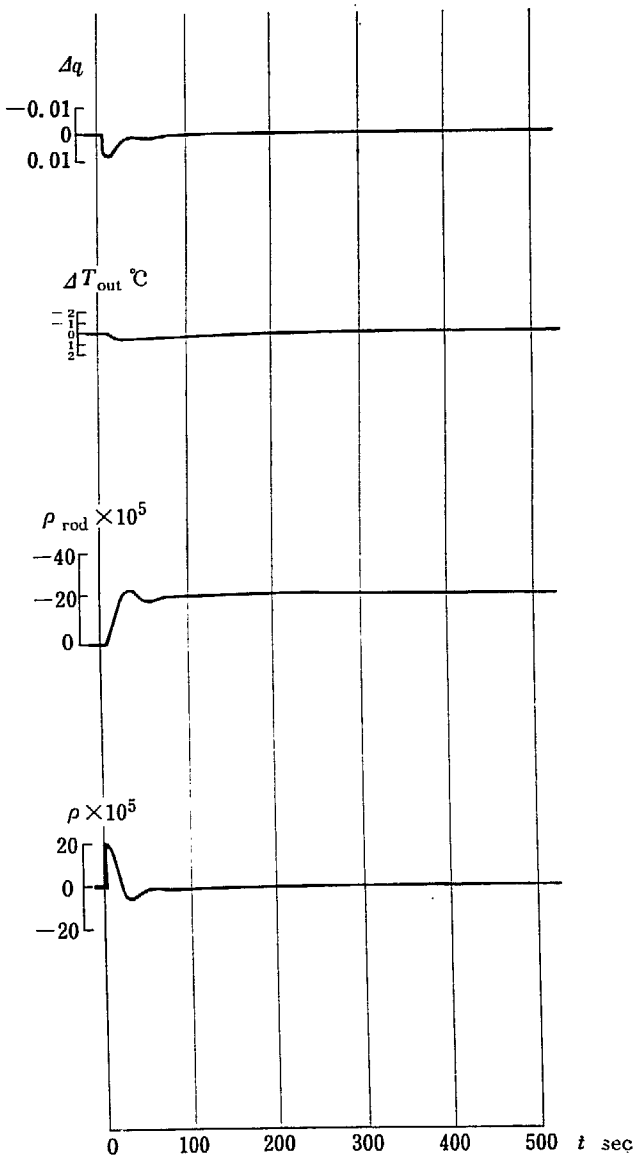

Fig. 4.17 (d) Examples of Transient Responses
$K=3\times10^{-6}$/sec °C
$K_{f2}=10^4$ °C $T_I=80$ sec $T_D=30$ sec $\rho_{ex}=2\times10^{-4}$

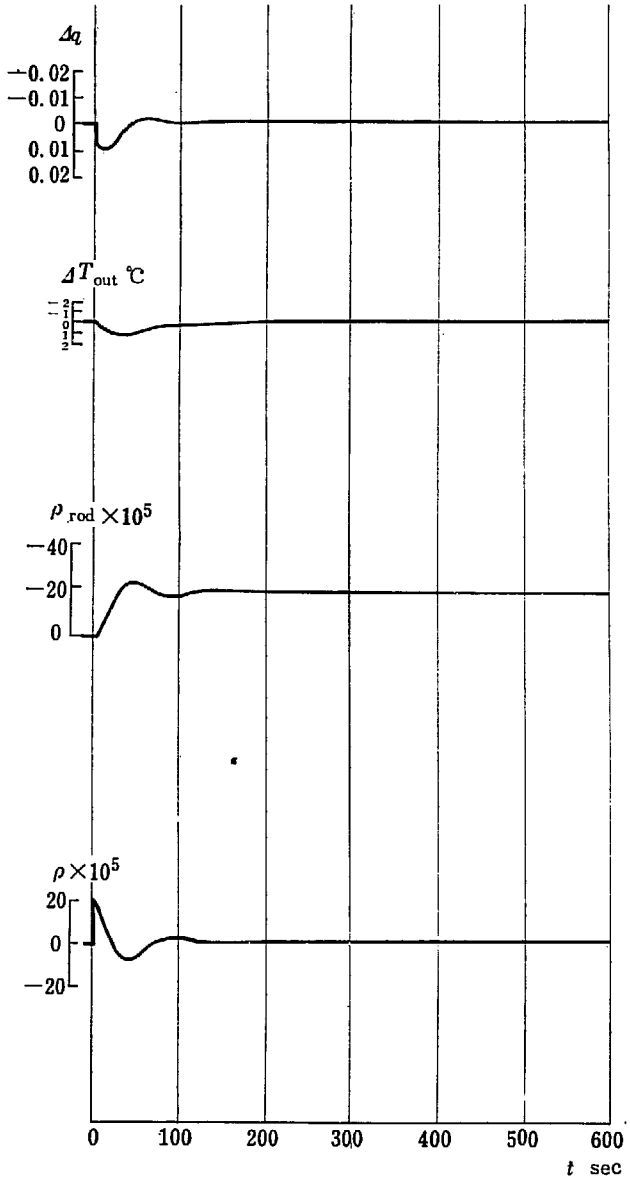

Fig. 4.17 (e) Examples of Transient Responses
$K=10^{-5}$/sec °C
$K_{f2}=10^4$ °C $T_I=80$ sec $T_D=30$ sec $\rho_{ex}=2\times10^{-4}$

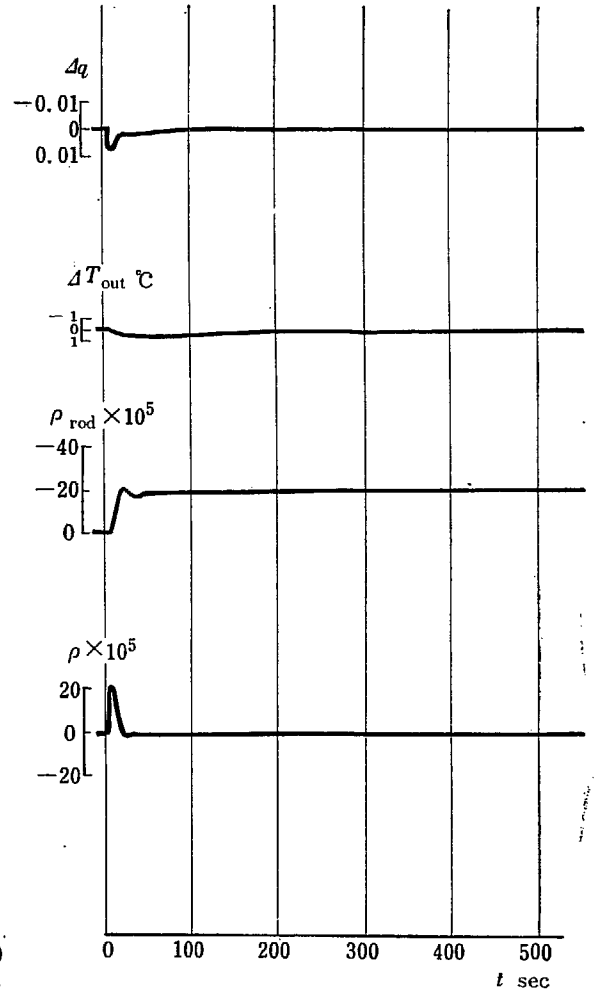

Fig. 4.17 (f) Examples of Transient Responses
$K=3\times10^{-5}$/sec °C
$K_{f2}=10^4$ °C $T_I=80$ sec $T_D=30$ sec $\rho_{ex}=2\times10^{-4}$

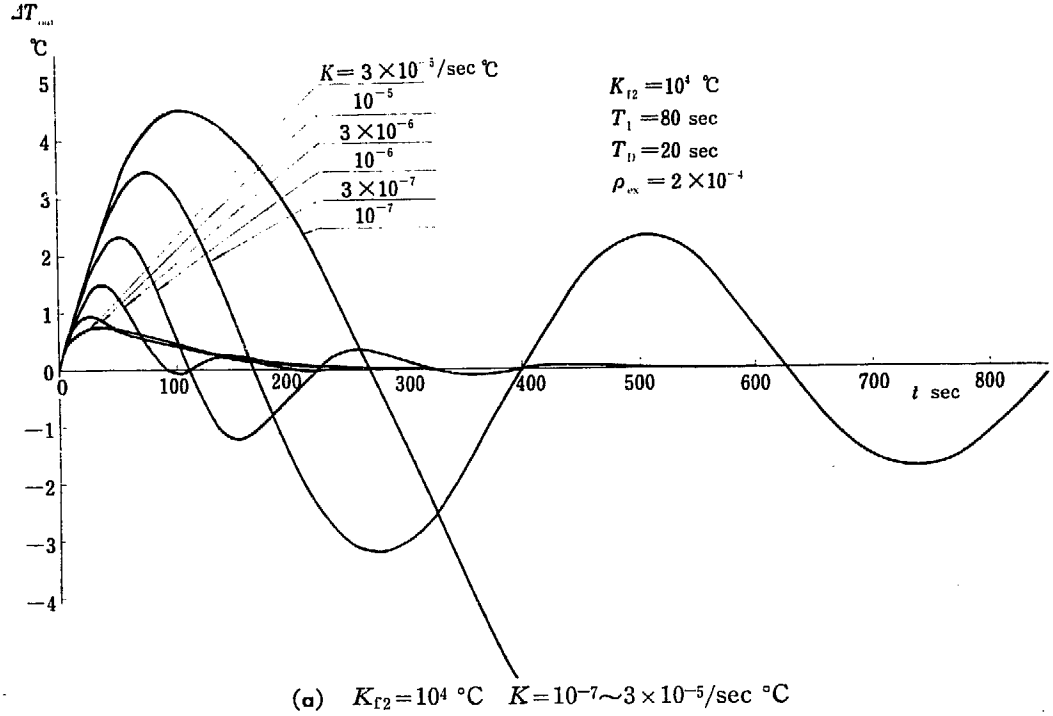

(a) $K_{f2}=10^4$ °C $K=10^{-7}\sim3\times10^{-5}$/sec °C

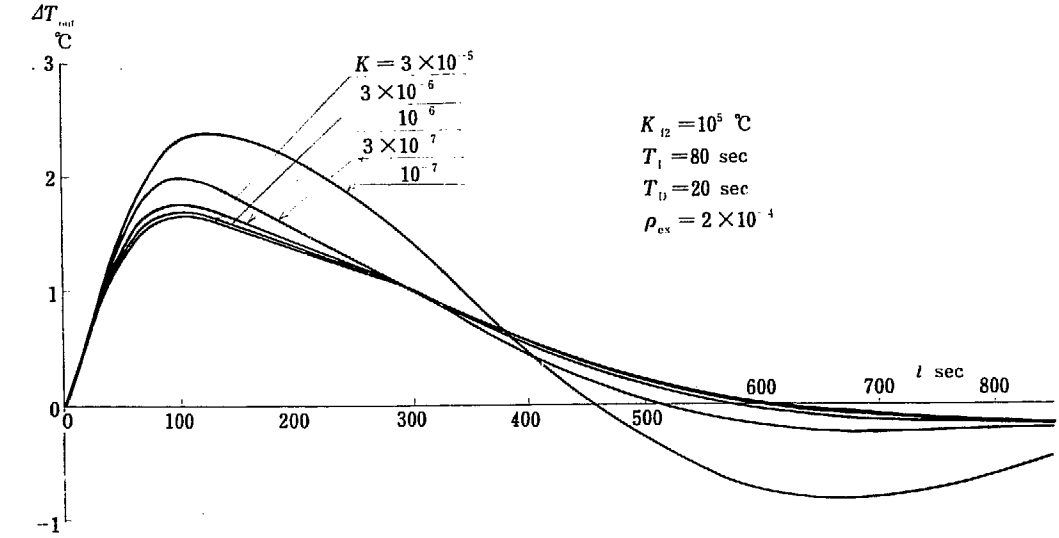

(b) $K_{f2}=10^5$ °C $K=10^{-7}\sim3\times10^{-5}$/sec °C

Fig. 4.18 Effect of Varying K on Response of ΔT_{out}
$T_I=80$ sec $T_D=20$ sec $\rho_{ex}=2\times10^{-4}$

as low as 10^{-7}/sec °C. On the other hand, if K_{f2} is large, the effect of varying K is not pronounced as shown in **Fig. 4.18 (b)**.

4.3.4 Effect of Rod Speed Limit

In **Fig. 4.20** is shown the effect of the limit in control rod speed. If the limit is larger than 1.9×10^{-5}/sec, the rod speed does not reach its maximum for a reactivity disturbance as much as 2×10^{-4}. If the limit is set at 5×10^{-6}/sec, the temperature overshoot is quite large, though still tolerable. If the rod speed limit is of the order of

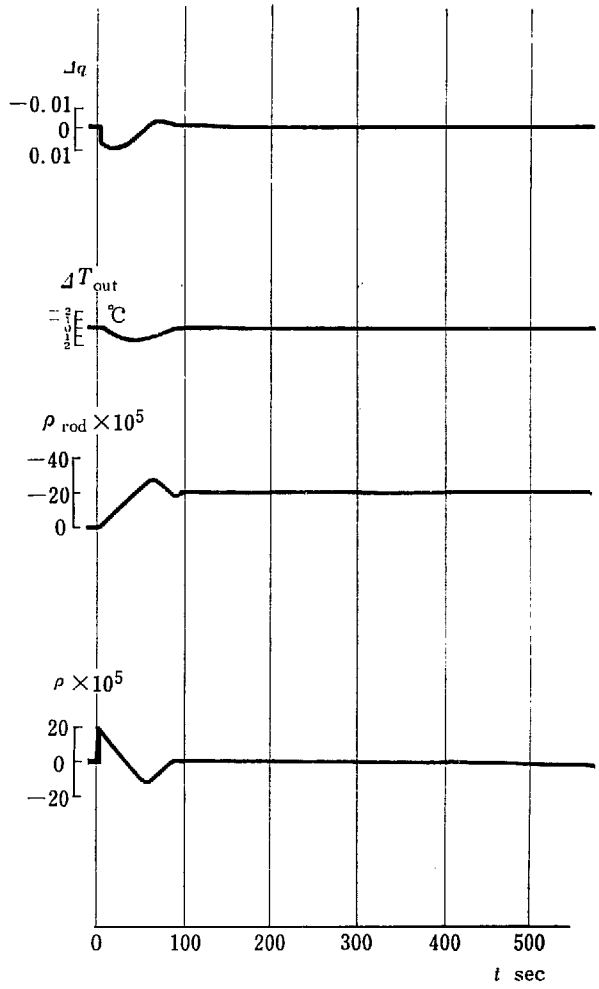

Fig. 4.19 Example of Transient Responses

$K=3\times10^{-5}$/sec °C $K_{f2}=10^4$ °C $T_I=80$ sec $T_D=20$ sec $\rho_{ex}=2\times10^{-4}$ $R_{max}=5\times10^{-6}$/sec

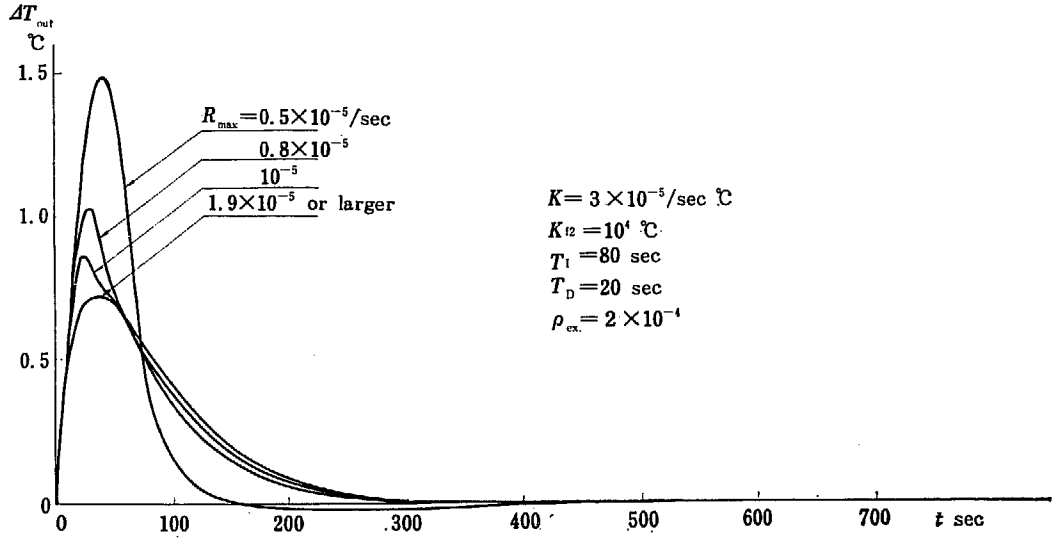

Fig. 4.20 Effect of Rod Speed Limit on Response of ΔT_{out}

10^{-5}/sec, it does not influence the system response significantly.

4.4 Comparison of the Optimum Responses

In **Fig. 4.21** comparisons are made between the optimum response of the continuous control system with and without the rod position feedback. The important features

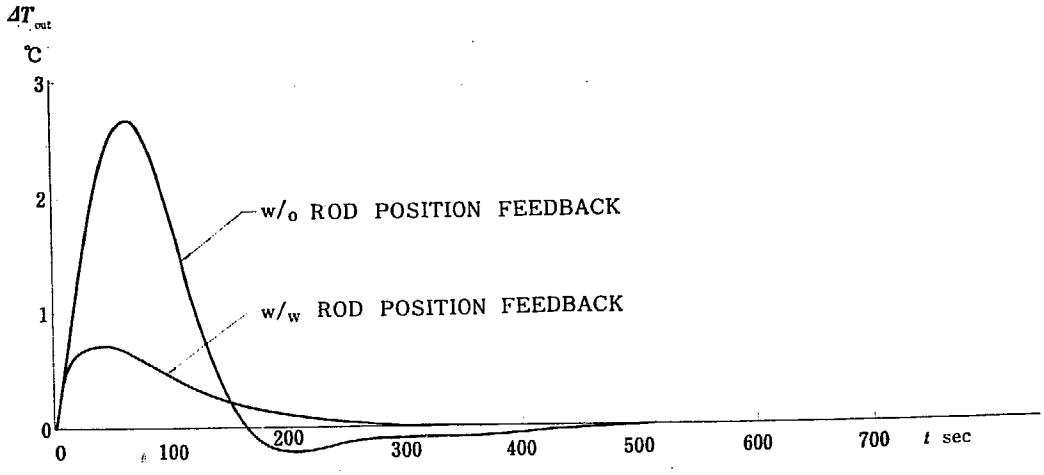

(a) Comparison of Optimum Responses of ΔT_{out}

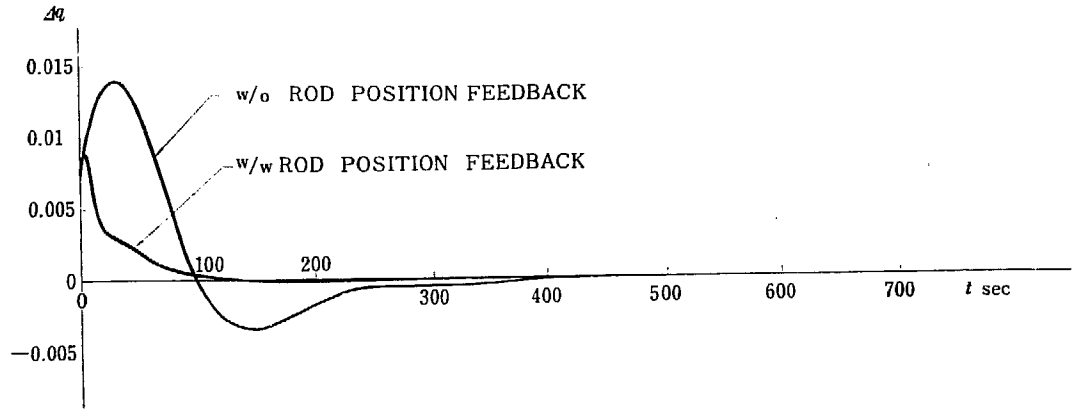

(b) Comparison of Optimum Responses of Δq

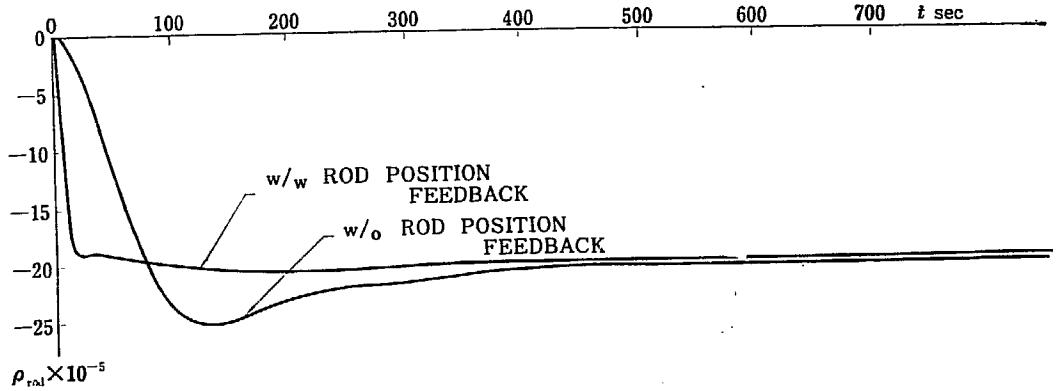

(c) Comparison of Optimum Responses of ρ_{rod}

Fig. 4.21 Comparison of Optimum Responses

Table 4.1 Comparison of Optimum Responses

System	T_I sec	T_D sec	K 10^{-5}/sec °C	K_f °C	Transient Peak in ΔT_{out} °C	Transient Peak in Δq %	Settling Time sec	Effects of Saturation in Rod Speed
w/o Position Feedback	∞	30	0.05	—	2.7	1.4	260	No effect if $R_{max}>10^{-5}$/sec
w/w Position Feedback	80	20	3	10^4	0.85	0.9	200	No effect if $R_{max}>2\times10^{-5}$/sec. Very little effect for $R_{max}=10^{-5}$/sec.

N. B. 1) Reactivity disturbance $\rho_{ex}=2\times10^{-4}$
2) Settling time is defined to be the time after which ΔT_{out} remains within ±0.1°C

of the two set of responses are compared in Table 4.1. From the figures and the table it is noted that the response of the system with feedback is better than that of the basic system, that is, the transient peaks of ΔT_{out} and Δq are smaller and the settling time is shorter. Although the comparison made here is restricted to a special case, for a particular controller setting and at a particular power level, it suggests that the rod position feedback might in general improve the system performance.

5. Conclusions

Stability analyses are made on the outlet gas temperature control system for British type power reactors, by means of the Nyquist's stability criterion and Kochenburger's describing function method. Transient responses are obtained by the analog computer and comparisons are made for different controller setups.

Numerical values of a reference reactor are used in computations. Five different types of controller are investigated; that is,

a) Continuous Control
b) Continuous Control with Saturation or Deadzone
c) Discontinuous Control
d) Continuous Control with Tachometer Feedback
e) Continuous Control with Rod Position Feedback

Applying the generalized Nyquist's criterion to the continuous control system, it is noted that there exist both upper and lower limits of controller gain for which the system is stable. In other words, the system is unstable for too low a gain due to the reactor instability and it is also unstable for an excessive gain due to controller forcing.

Generally speaking, the rate action is favorable for the system stability, while the reset action is not. The controller setting, $T_I=\infty$ and $T_D=30$ sec, seem to be optimum. For this setting the stable region of the controller gain is almost three decades (55 db), which is the largest of all the settings examined.

Varying the controller gain K the transient responses are compared for the

optimum controller setting described above. The optimum value of K is found to be 5×10^{-7}/sec °C, for which the gain and the phase margins are 26 db and 50 degrees, respectively.

Qualitative analysis is made on the effects of controller non-linearities by means of the describing function method. It is concluded that if the system contains saturation, the system is not controllable for a very large disturbance and diverges, and that if it contain a deadzone, it is possible to adjust the controller gain so that the system does not diverge, but a limit cycle is inevitable.

Transient responses following a reactivity change of 2×10^{-4} are compared, introducing saturation of the control rod speed into the continuous control system. It is observed that if the limit, R_{max}, is larger than 0.34×10^{-5}/sec, the saturation does not influence the responses. If the limit is lowered to 10^{-6}/sec, the responses become quite poor. The reasonable value of the limit to be used in actual reactors will probably be of the order of 10^{-5}/sec and hence it will little affect the response unless an excessive amount of disturbance is applied.

Kochenburger's describing function method is applied to the discontinuous control system. It is concluded that if the controller gain is very low the system diverges and that if otherwise the system undergoes sustained oscillations corresponding to stable limit cycles for disturbances of a moderate magnitude and it diverges for a very large disturbance.

Assuming the controller setting $T_I=80$ sec and $T_D=30$ sec, it is noted that if the controller gain is lower than 4.5×10^{-7}/sec, the system always diverges.

If the controller gain is between 4.5×10^{-7}/sec and 2×10^{-5}/sec, one stable limit cycle exists, while for the controller gain higher than 2×10^{-5}/sec there exist two stable limit cycles. In both cases the system diverges for a very large disturbance.

Analog computer studies are made for the same controller setting. The limit cycles are observed. The amplitude and the frequency of oscillation for different values of controller gain are compared. It is concluded that the describing function method is too crude an approximation to estimate the amplitude and the frequency of oscillation, although this method is useful for qualitative analysis, that is, for determinations of stability, existence of the limit cycles and so on.

The maximum aliowable disturbance is obtained as a function of the controller gain. It is almost proportional to the controller gain. The system diverges for a disturbance larger than 10^{-4}, if the controller gain is set at 10^{-6}/sec. If the controller gain is increased to 10^{-5}/sec, the system is stable, unless the disturbance exceeds 10^{-3}. Hence it is not advisable to use a lower controller gain in the discontinuous control system.

The conditions of stability for the continuous control with tachometer feedback are essentially the same as those for the basic continuous control system except minor changes in the parameters.

Stability of the control system with rod position feedback is also investigated.

It is concluded that there exist both upper and lower limits of the controller gain as there are for the basic continuous control system. The stable region is, however, larger for this system, namely, more than three decades (approximately 70 db).

The optimum controller setting is found to be T_I=80 sec and T_D=20 sec in this case. The optimum controller gain is 3×10^{-5}/sec °C and the feedback gain of 10^4°C is optimum.

The effect of saturation of the rod speed is also studied. It is noted that the saturation has no effect if the limit is larger than 1.9×10^{-5}/sec. The temperature transient is still tolerable even for $R_{max}=5\times10^{-6}$/sec.

Comparisons are made between the optimum responses of the basic system and the system with the rod position feedback. It is noted that the latter has better performances, a shorter settling time and a smaller temperature overshoot. This fact indicates that, as far as these comparisons are concerned, the introduction of the rod position feedback improves the system performance.

The analysis in this report is restricted to the reactor control system and the effect of the secondary system is not taken into consideration. A one point, lumped parameter model is used to simulate the reactor. These assumptions are considered to give sufficient results for the control system design.

In order to obtain more detailed results and to justify these assumptions the analysis should be developed in future to inclued the effects of the secondary system and to take the space dependent kinetics of reactor into consideration.

Although this analysis refers to a particular reactor at a particular power level, the results described here may be considered to provide with general guides for the analysis and the control system design of the reactors of this type.

Acknowledgement

The Authors thank Mr. MASAO HARA who gave them assistance in using the PACE analog computer.

Reference

1) J. MIIDA *et al.*: JAERI-1006-B (1959).
2) T. J. O'NEILL: Geneva Conf. P/21 (1958).
3) R. J. KOCHENBURGER: Trans. AIEE **69**, 687 (1950).
4) H. CHESTNUT *et al*: Servomechanisms and Regulating System Design, John Wiley (1951).
5) J. MIIDA *et al*: *Automatic Control*, **7** (3), 14 (1960)——in Japanese.
6) K. IZAWA *et al.*: Regelungstechnik, Moderne Theorie und ihre Verwendbarkeit, R. Oldenbourg, München (1957) pp. 294-300.
7) J. MIIDA *et al.*: *Nucl. Sci. Engg.*, **11**, (1), 55, (1961).

Table Contents

Figure Contents